Review Article

ADVANCES IN SOLAR RADIATION ESTIMATION TECHNIQUES: A COMPREHENSIVE REVIEW

Feyza Nur YEŞİL[1,*], *Tuba Nur SERTTAŞ*[1]

[1]Department of Electrical and Electronics Engineering, Faculty of Technology, Afyon Kocatepe University, Gazlıgöl Street, Afyonkarahisar, Turkey

fyesil@aku.edu.tr, tngul@aku.edu.tr

[*]Corresponding author: Feyza Nur Yeşil; fyesil@aku.edu.tr

DOI: 10.15598/aeee.v22i4.5732

Article history: Received Feb 2, 2024; Revised Aug 21, 2024; Accepted Aug 28, 2024; Published Dec 31, 2024.

Abstract. *Solar energy is a favored renewable energy source in the energy sector due to its zero emissions, environmental friendliness, low cost, and sustainability. However, meteorological factors such as weather conditions and cloud movements can interrupt solar radiation, potentially leading to undesirable outcomes in the energy sector. Solar irradiance forecasting is crucial for mitigating these adverse effects and supporting the development of renewable energy projects. In this study, the methods employed in the literature for various prediction intervals are classified, and the evaluation results of these predictions are summarized in a table. Also, an example model created with ANFIS for estimating solar radiation is presented. Image-based and NWP models is perform well for short-term forecast horizons. To predict various time horizons, artificial intelligence-based models such as time series models, deep learning, and machine learning are prefer. Hybrid models that combine multiple methods to achieve higher accuracy are also proposed, although this increases the complexity and cost of the model. There are potential limitations in the field of solar forecasting that arise from model and data characteristics. Therefore, This study aims to guide other researchers in this field by discussing the features, limitations, and results of the models used for solar forecasting. Also, the example of daily solar radiation forecasting provided in this study offers a practical application opportunity for researchers new to this field.*

Keywords

ARIMA, hybrid, LSTM, NWP, solar irradiance predict.

1. Introduction

Today, the increasing demand for energy, coupled with the growing world population, has highlighted the need for renewable energy sources. The negative effects of fossil fuels, such as global warming, air pollution, and health problems, have made renewable energy sources an attractive alternative [1]. Unlike conventional sources, naturally occurring solar, wind, hydroelectric, geothermal, and biomass energies are renewable and sustainable. Consequently, many countries are adopting these sources to achieve energy independence [2]. Solar energy, which occupies a significant part of the energy market, is one of the most preferred sources in the renewable energy sector [3]. When solar radiation reaches the Earth's surface, only 70% of this radiation is absorbed, while the remaining 30% is reflected and emitted into space. The total amount of energy absorbed by the Earth's surface is greater than the combined reserves of coal and oil [4]. Solar energy is a long- term, low-cost, environmentally, friendly, and inexhaustible resource [5]. However, due to its intermittent nature, the output power is variable which can be defined as a non-stationary time series [6].

A solar photovoltaic module is a panel that can convert solar radiation directly into electrical or thermal energy, or both [7]. Solar panels have gained popularity

because they can be easily integrated wherever there is sunshine, without the need for long power lines, and they require little maintenance [8]. However, they have the problem of unpredictability, as weather conditions change throughout the year [9]. Since the sun has an intermittent energy structure, forecasting the output power of photovoltaic (PV) systems becomes difficult. Therefore, additional measures are needed to mitigate the impact of energy intermittency and surges in the utility sector, such as excess electricity generation [10]. Accurate solar radiation forecasts are essential for conducting feasibility studies on energy systems [11]. One of the fundamental parameters used to estimate the total energy production of a PV plant is the measurement of solar radiation values over time [12].

Total solar radiation is attenuated by atmospheric interaction as it travels towards the Earth's surface. It has two components: Diffuse Horizontal Irradiance (DHI) and Direct Normal Irradiance (DNI). The Global Horizontal Irradiance (GHI) is obtained by summing these two components [13]. Generally, GHI estimation can be divided into very short-term, short-term, medium-term, and long-term horizons [14]. The input variables used in the solar radiation forecasting model determine the forecast horizon [15]. There are three main techniques for solar radiation forecasting: Numerical Weather Prediction (NWP), image- based forecasting and statistical models [10]. The relationship between forecast horizon and forecast method is shown in Tab. 1. Approaches developed for solar radiation forecasting can be categorized into two main types: numerical methods and statistical methods. Numerical methods are based on the principle of reproducing a physical phenomenon, while statistical methods rely on machine learning, time series analysis, sky models, and satellite-based derived from past time series analysis [15].

Tab. 1: Relationship between forecasting horizon and forecasting method.

Forecasting horizon	Time horizon	Forecasting method
Very short-term	A few seconds–one hour	Image-based
Short-term	One hour–a few hours	Image-based, NWP
Medium-term	A few days–one week	NWP, Statistical
Long-term	One week–one year	Statistical

The aim of this paper is to review the methods used in the literature to estimate solar radiation and analyze the findings. By presenting the techniques of the different methods in a clear and comprehensible manner, a summary table will be created to facilitate comparison between the methods. This review will enhance the understanding of the methods and offer guidance for future applications. Additionally, an example sunlight prediction model is included for researchers who are new to this field. The organization of this article is as follows. Solar radiation forecasting methods are classified into three main categories. Section 2 deals with Image-based models, Section 3 deals with NWP models, Section 4 deals with statistical models, and Section 5 with hybrid models. An example of solar irradiance forecasting generated by the Adaptive Neuro-Fuzzy Inference System (ANFIS) model and tables presenting the results used to analyze the performance of forecasting techniques proposed in the literature are found in Section 6. This section also discusses the limitations in the field of solar forecasting. The conclusion presents a summary of the literature on the methods and includes a discussion section.

2. Image-based models

Cloud motion has a significant impact on the estimation of solar radiation as the position of clouds can obstruct the sun. Since clouds are variable, they play a key role in determining the models developed for forecasting [10]. Cloud motion data from satellite imagery and ground-based sky imagers are often important inputs for short-term forecasting [16]. Figure 1 demonstrates a straightforward flow diagram of the image-based solar forecasting method.

2.1. Satellite images

Satellite imagers capture images of large areas multiple times within an hour and record them spatially and temporally [17]. Solar radiation estimation is based on cloud motion vectors (CMVs) derived from images captured by these satellites [18].

For very short-term forecast horizons, the use of satellite imagery is more suitable. A forecasting algorithm has been developed for the Dutch region using the physical properties of clouds obtained from the Spinning Enhanced Visible and Infrared Imager (SEVIRI) on the Meteosat Second Generation Geostationary Satellite. The novelty of this paper lies in deriving cloud motion vectors through the analysis of the physical characteristics of clouds. A forecast horizon of 0-240 minutes is defined for the DNI and GHI forecasts. It has been shown that the SEVIRI forecast model for July 2017 achieves better results than the HARMONIE NWP model, and it has been found that an accurate forecast depends on weather conditions [18].

The interruption of solar radiation measurement in certain regions degrades the accuracy of forecasting. To address this issue, the study utilizes data from

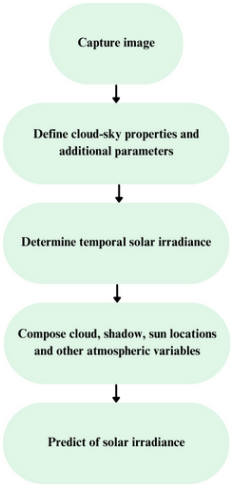

Fig. 1: A simple flowchart illustrating image-based forecast.

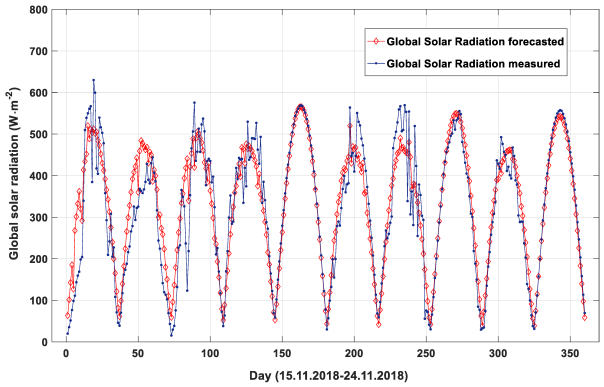

Fig. 2: The forecasted results of GHI under all condition days with a 60 min horizon [19].

AGRI sensors on the FY-4A satellite to estimate GHI in the Northwest China region under various weather conditions. This estimation is based on the cloud index methodology (CSD-SI). The calculation process is simple because this method does not require historical or observational data. This makes it well-suited for desert regions where measurements are not always available. A forecast horizon of 15-180 minutes is defined. Figure 2 shows the solar irradiance forecast results for a 60-minute forecast horizon under all sky conditions. The best forecast performance is achieved under clear skies [19].

In another study, the same author developed an algorithm to estimate surface solar radiation in very short-term intervals (30-180 minutes) using AGRI sensors on the FY-4A geostationary satellite. GHI and DNI forecasting results are compared for four typical months, representing the four seasons, using meteorological data from the Chinese region. The GHI forecasting results of the FY-4A-AGRI model showed the best results in all months and time horizons [20].

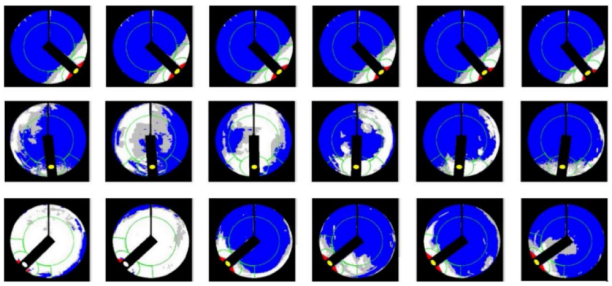

Fig. 3: TSI images captured with 10-min intervals for three scenarios: morning (top), day (middle), and evening (bottom) [24].

Solar radiation estimation varies with sky conditions, and the accuracy of the estimation decreases during cloudy sky situations. A dataset from the Geostationary Operational Environmental Satellite (GOES) and Heliosat-2 satellites were utilized as input to enhance the estimation of solar radiation during cloudy sky conditions in French Guiana. The novelty of this work lies in the integration of a cloudy sky with a radiative transfer parameterization (RTP) to gain a deeper understanding of the properties of local clouds. This combination has been shown to yield better results in regions with significant cloud cover [21].

2.2. Ground-based sky imagers

Sky image-based forecasting models can better identify local sky information, such as sun position or cloudiness, compared to satellite-based forecasting models [22]. Most of the cameras used have fisheye lenses that can capture the entire sky, allowing for the analysis of the position, movement, and optical properties of clouds [23]. Images captured by ground-based upward-looking sky cameras, such as the Whole Sky Imager (WSI) and Total Sky Imager (TSI), are used to model solar radiation prediction [24]. Solar radiation forecasting for Oklahoma utilizes sky images taken by TSI every 10 minutes. Figure 3 shows the RGB (Red-Green-Blue) cloud image captured in the morning, noon, and afternoon, illustrating a 10-minute variation. The black region is negligible because of the shadow cast by the camera assembly. The blue color represents a clear sky, while the white color represents a thick cloud, and the lighter blue color represents a thin cloud. Green regions indicate special areas [24]. In models based on sky imagery, forecast performance is affected by convergent ray projection errors, stray light, and noise, which make cloud detection difficult. To address this issue, a testbed for a virtual sky imager was created in this study. This virtual testbed has been observed to greatly improve performance, as it can detect individual cloud detection errors [25].

One of the challenges faced in image-based solar forecasting is the misclassification of cloud-sky types and inadequate extraction of cloud features. In order to effectively implement the cloud-sky identification process, this study proposes a clustering-boundary correction algorithm to address this issue. It aims to extract multidimensional features from all-sky images, including both regional and global features [26]. A methodology is presented that combines real-time irradiance and All-Sky imagery values for a very short-term forecast in Salto, Uruguay. Solar forecasting is performed by considering the average movement of clouds. The proposed model is evaluated for clear, cloudy, and partly cloudy days, and its performance under various conditions is observed. Favorable forecasting skills were obtained under partly cloudy and highly variable conditions [27]. Taking only the average speed of the clouds has a negative impact on forecast performance because clouds at different altitudes have varying speeds. Therefore, in the study conducted for the city of Wollongong, Australia, an alternative methodology was developed instead of simply calculating the average speed of the clouds. A model for short-term solar radiation forecasting is created by considering the individual movements of clouds, their height above ground level, and cloud thickness. The proposed model does not require historical data and can detect the velocities of clouds in various layers. Figure 4 shows the solar irradiance results for forecast time horizons of 1, 5, and 15 minutes. Using the proposed model, an accuracy of 81% is achieved for a 1 minute forecast time horizon. It is concluded that classifying clouds based on their levels and tracking the motion of individual clouds improves forecast performance [28].

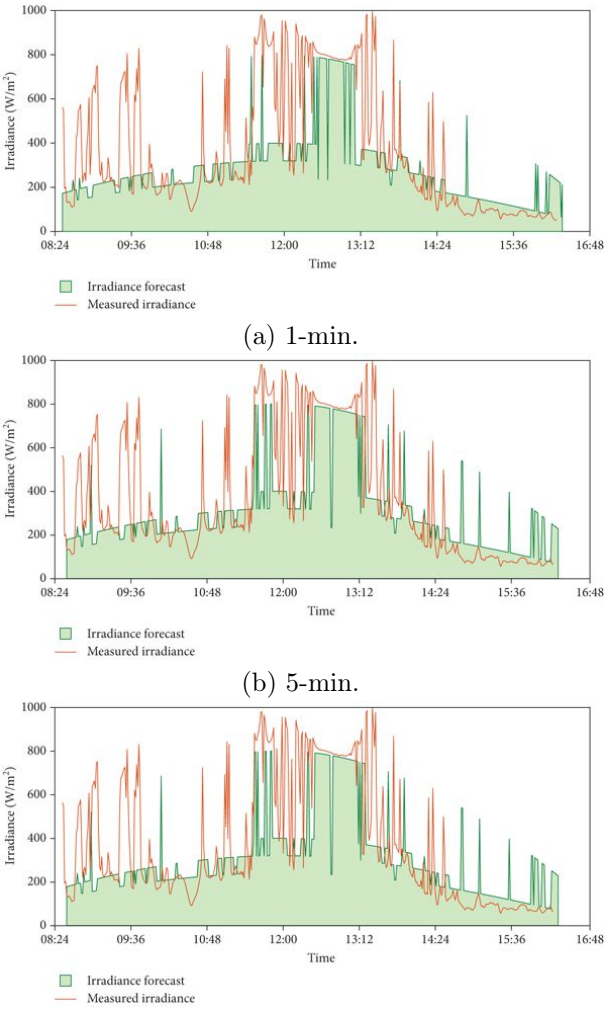

Fig. 4: The solar irradiance results for forecast time horizons of (a) 1-min, (b) 5-min, and (c) 15-min [28].

Cloud distribution and thickness in sky images are important parameters for solar forecasting. Images obtained from the all-sky imager are used to infer cloud characteristics in the short-term solar radiation forecast for the Taiwan region. With the proposed new cloud feature extraction method, sky images are analyzed and weighted regionally and globally. These weight parameters are used as input data for the Long Short Term Memory (LSTM) in the training model. In this way, the effects of cloud distribution and cloud thickness parameters are included as determinants in solar forecasting [29].

All Sky Imager systems vary in their camera characteristics, cloud distribution and algorithms, algorithms and solar forecasting approaches. Four all-sky imagers based on different methods were used for solar radiation forecasting in Spain. Solar forecasting was conducted for a duration of 1 to 20 minutes, taking into account different weather conditions. All ASIs performed with an Root Mean Squared Error (RMSE) ranging from 6.9% to 18.1% [30]. There is a lack of studies in the literature on extracting spatio-temporal

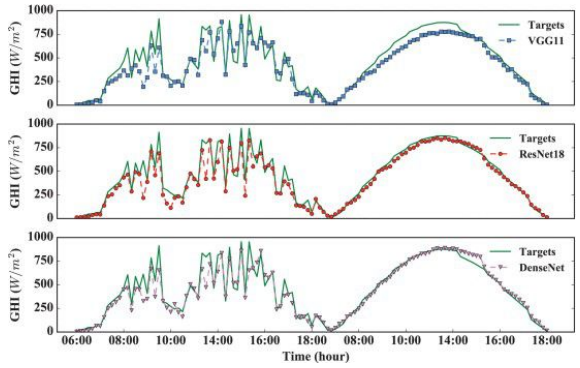

Fig. 5: Forecast results of VGG-11, ResNet-18, and DenseNet-121 [32].

information from sky images. Therefore, in this study, a Cuboid method is proposed to define the spatio-temporal features of grayscale sky images, and a pool of spatio-temporal information is created. Thanks to the dynamically and statically extracted spatio-temporal features, a superior estimation performance is achieved compared to other object detection methods, such as DenseNet [31]. In another study where space-time information was used to enhance prediction accuracy, the DenseNet method demonstrated superior prediction performance compared to other ResNet models. The forecast results for the next two days are presented in Fig. 5 [32]. Deep learning-based approaches alone involve costly and complex mathematical calculations. Using multiple inputs significantly increases the computation time. To solve these problems, this study utilizes k-Nearest Neighbors (k-NN) and Random Forest (RF) machine learning models with dimensionality reduction techniques. Feature extraction is achieved by analyzing the sky images captured by the all-sky imager and total sky imager. The results of the sun prediction using the proposed training model show that it outperforms the deep learning-based approach [33]. In another study utilizing machine learning algorithms, a model based on the principle of real-time surface irradiance mapping was developed to correlate sky images with solar irradiance values. Red-Green-Blue (RGB) values and pixel location information are extractes from sky images. The trained model is continuously updated and used for very short-term (one-minute to ten-minute) forecast horizons. It has been observed that the prediction method using Back Propagation Neural Network (BPNN) and Support Vector Machine (SVM), based on pixel information input, better tracks the variation of irradiance under different cloud conditions [22].

3. Numerical weather prediction models

The mathematical analysis of the equations that physically describe the changes occuring in the atmosphere, the weather, constitutes, the NWP models [34]. At short-term forecast horizons, such as a few days ahead, NWP models demonstrate superior forecast performance [35]. While NWP models perform well for large scale processes, they parameterize atmospheric phenomena that they cannot determine at small scales [36]. NWP models can be categorized into global models and regional or medium-scale models [37].

For cloudy days, deviations the forecast of the DNI forecast with NWP models can be larger. To enhance the accuracy of hourly DNI forecasting in the Southern Great Plains region, Texas integrated the Wheather Research and Forecasting with Solar Extension (WRF-Solar) model with the Fast All-Sky Radiation model (FARMS-DNI). This significantly reduced the effects of uncertainty in cloud information [38]. The study proposes the use of the WRF model to forecast hourly solar radiation for Gifu city in Japan. When comparing the results of the medium- scale model with those of the LSTM model, it is evident that the proposed model demonstrates a prediction capability with 19% less error [39]. The WRF model, which is used for hourly solar radiation forecasting in the Singapore region, is combined with multivariate statistical learning techniques such as stepwise variable selection and alternative dimensionality reduction. This combination aims to achieve accurate forecasting with minimal error [40]. In another study, the same author attempted a novel approach by integrating NWP models with post-processing algorithms. The regression models used to forecast monthly solar radiation in Pennsylvania were combined with the NWP post-processing algorithm. With NWP post-processing, the prediction models were shown to perform with higher accuracy [41]. In the Desert Rock region, high-resolution models are used for a forecast horizon ranging from 1 to 12 hours. It is emphasized that the use of numerical weather forecast information produced by space centers and weather forecasting agencies is crucial in solar energy applications. Figure 6 shows the marginal distributions of forecast and observation for the three Numerical Weather Prediction (NWP) models across seven regions in 2020. The HRES model demonstrates the best agreement between the forecast and observed marginal. The forecasts of the ECMWF-HRES model showed the best performance with an RMSE of 14.0-33.7% [42]. In the study on hourly solar radiation forecasting in Australia, the forecasting capabilities of NWP models using the Earth System Simulator (ACCESS) and the Global Forecast System (GFS) were examined [43].

The forecast performance NWP models may decrease as the forecast horizon increases. The NWP information used to perform short-term solar radiation forecasting in Goodwin Creek, Mississippi, is updated hourly. The novelty of this study lies in the utilization of a Kalman Filter to eliminate the inherent bias effects of the NWP model. The findings demonstrate that the NWP method with the Kalman Filter is able to forecast with fewer errors [44].

4. Statistical models

The preferred statistical models for different forecast horizons are artificial neural network-based models and time series models that incorporate historical irradiance data.

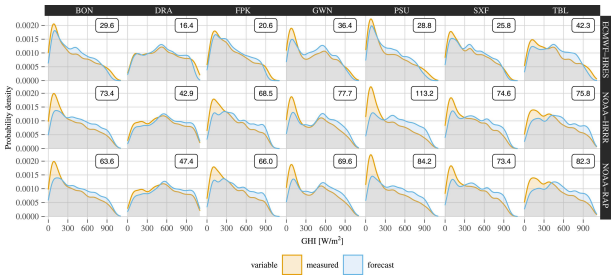

Fig. 6: Marginal distributions of forecast and observation, from three NWP models, at seven locations, over the year 2020 [42].

4.1. Auto regressive integrated moving average

In solar forecasting, the time series model uses historical data of the irradiance value to infer its future behavior [45]. Autoregressive Moving Average (ARMA) model is preferred for autocorrelated time series data. In the ARMA model, "AR" stands for the autoregressive part, while "MA" stands for the moving average part. The model is denoted as ARMA (p,q). In the symbolic representation, "p" represents the degree of the autoregressive part, and "q" represents the degree of the moving average part [46]. By extending the ARMA method, Seasonal Auto Regressive Integrated Moving Average (SARIMA) and Auto Regressive Integrated Moving Average (ARIMA) models are obtained [47]. In the equations provided below to represent ARIMA model variants, $\mathbf{Y}_t$ represents the time series, **c** denotes any constant, p indicates the number of lags relative to $\mathbf{Y}_t$, **q** signifies the number of past error terms, and e_t represents white noise.

Equation for a p-th order AR(p) model is represented as:

$$Yt = c + et + \sum_{i=1}^{p} \Phi i Yt - i \tag{1}$$

Equation for a q-th order MA(q) model is represented as:

$$Yt = c + et + \sum_{i=1}^{q} Qiet - i \tag{2}$$

Equation for p-th and q-th order ARMA(p,q) model is represented as:

$$Yt = c + et + \sum_{i=1}^{p} \Phi i Yt - i + \sum_{i=1}^{q} Qiet - i \tag{3}$$

Equation for ARIMA(p,d,q) model is represented as:

$$\Delta Yt - i + 1 = Yt - i + 1 - Yt - i \tag{4}$$

$$Yt = Yt - 1 + et + \sum_{i=1}^{p} \Phi i \Lambda Yt - i + 1 + \sum_{i=1}^{q} Qiet - i \tag{5}$$

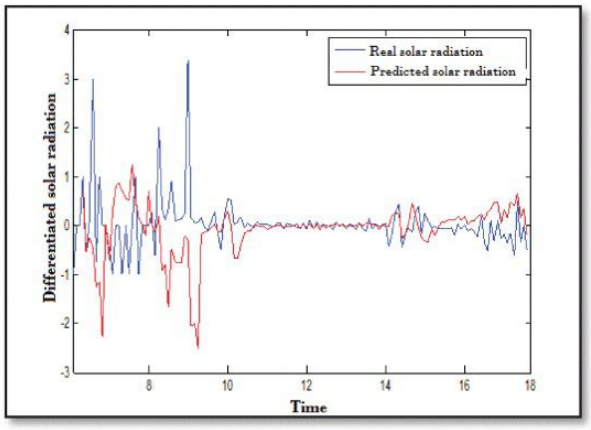

Fig. 7: Solar irradiance forecasting for a winter day by ARMA [49].

For an accurate solar radiation forecast, a dataset covering at least one year is required. Shadab et al. used monthly solar irradiance values for a total of 34 years between 1984 and 2015 for monthly solar radiation forecasting in Delhi, India. An optimal seasonal ARIMA model, based on the Box-Jenkins methodology, was developed for a single region [45]. In their next study, a seasonal ARIMA model was created for more than one region in the city of Delhi. It was aimed to identify regions with high solar potential and to give ideas to energy investors [48].

The solar potential varies according to the climatic conditions of different geographical locations. ARIMA models were specified for different climatic conditions to forecast monthly solar radiation for Jordan and Poland. All the proposed models predicted with R^2 values above 85%. The SARIMA model developed for the Jordan region showed the best prediction performance in the GHI estimation for August in the summer season. This is because the solar radiation behavior in the Jordan region tends to be more stable [11]. During the winter season, solar radiation can be intermittent, leading to a decrease in forecast performance. An ARMA model is developed for daily solar radiation forecasting for North Barcelona in winter. The prediction plot in Fig. 7 shows that the ARMA model effectively predicts small changes in irradiance [49].

Solar forecasting performance is influenced by seasonal conditions as well as the change of weather conditions during the day. Hourly solar radiation forecasting is performed for the city of Missour, Morocco considering four different weather conditions. LSTM and Multilayer Perceptron (MLP) models outperformed the SARIMA model, while the SARIMA model also performed effectively in clear and less variable weather conditions [50].

ARIMA-based time series models show better performance for long-run forecast horizon. A Seasonal

ARIMA model was developed to forecast monthly and daily solar radiation for Seoul, South Korea [51]. The SARIMAX model is developed for forecasting daily and monthly solar irradiance in Islamabad, Pakistan, using multiple input values. Both ARIMA-based models obtained a more successful result for the long-run forecast horizon [52].

Studies comparing ARIMA-based models with machine learning models are also frequently found in the literature. ARIMA and Fuzzy Logic (FL) models were proposed for forecasting hourly DNI in Golden, Colorado. When comparing the results, the FL model predicted with less error [14]. In the hourly GHI forecasting for Brazil, the proposed ARIMA model was not superior to machine learning based models [53]. However, the fact that the proposed ARIMA model for Jaffna, Sri Lanka outperforms the Neural Networks, Random Forest Tree (RF), SVM, and Linear Regression (LR) models in DNI forecasting suggests that this assumption is not always valid [54]. The ARIMA model proposed as an hourly solar irradiance prediction model for Tetouan, Morocco also outperformed SVM and the k-NN machine learning models [55]. The same author proposed the ARIMA model for forecasting daily and monthly solar radiation in Morocco [7, 56]. The performance of ARIMA models can be affected for better or worse depending on the input variable, forecast horizon and seasonal characteristics. Paulescu et al. summarized this situation in their study by arguing that no model can be characterized as the best. However, the features that contribute to a model's superior performance compared to others are controversial [57].

4.2. Artifical neural network

The working principle of Artificial Neural Networks (ANN) is based on the functioning of biological nerve cells. It is modeled by mathematically expressing the structure and functions of biological neurons [58]. Each input parameter is weighted, then summed, and the outcome is transformed into a transfer function, such as sigmoid, hyperbolic, or tangent, according to the operating principle of an artificial neural network [59]. ANN is one of the most preferred approaches in solar energy applications [60]. It performs prediction using algorithms such as feed-forward and feed-back propagation [61].

The structure of an artificial neuron was illustrated in Fig. 8. The net input is obtained by adding the activation threshold to the weighting of neighboring artificial neurons. The activation threshold can have a positive or negative value. The output value is calculated by applying the activation function to the net input data. The equations used in the process are provided below [62].

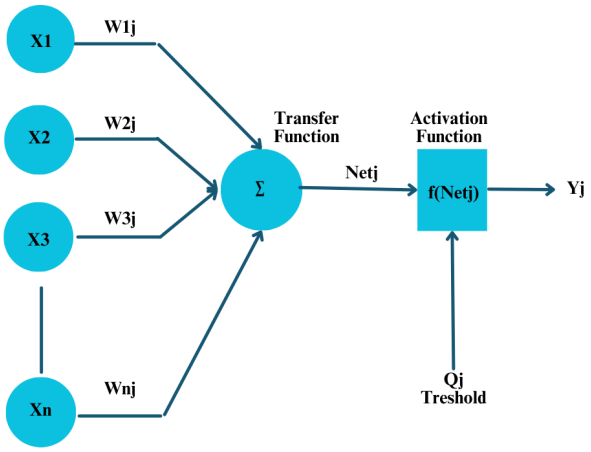

Fig. 8: Structure of an artificial neuron.

$$Netj = \sum_{i=1}^{n} XiWij - Qj \tag{6}$$

$$Yj = f\left(\ Net \quad j \ \right) \tag{7}$$

The back-propagation (BP) algorithm continuously updates the output value, minimizing the error level and bringing it closer to the target value. Among feedback networks, one of the simplest structures trained with the standard BP application is the Elman network model [63]. The proposed ANN for forecasting monthly solar radiation in Chandigarh, India is trained using the Elman back-propagation algorithm. The decimal normalization technique was used for data preparation. The Elman BPNN showed better prediction performance than the feed-forward neural network [64]. One of the BP application types is the momentum and learning fold BP algorithm. The difference from standard BP algorithms is the use of weight coefficient values before two iterations. A neural network model trained with momentum and learning coefficient BP algorithm is proposed to perform daily solar radiation forecasting for the city of Aswan, Egypt. It predicted with less error than the standard BPNN model [65]. Another type of BP algorithm is the Levenberg Marquand training algorithm. The Levenberg Marquand BPNN model developed for hourly solar irradiance forecasting for Surabaya, Indonesia showed a prediction performance with an R^2 value of 0.983 [66].

In the literature, linear models based on experiments and observations have also been developed for solar radiation forecasting. The Angstrom-Prescott type linear model and the Levenberg Marquand BP algorithm network method, developed for daily solar radiation forecasting in Mersin, Turkey, were compared [67]. Another study compared the Angstrom-Prescott type linear model and Levenberg Marquand BP method for monthly solar irradiance forecasting for another city in Turkey, Antakya [68]. In both studies, it was observed

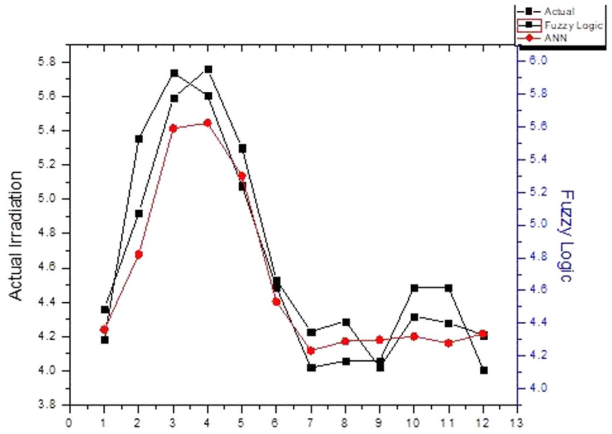

Fig. 9: Comparison graph of ANN and Fuzzy logic [8].

that the proposed ANN model obtained a better prediction result. In another study comparing empirical and ANN models, the BPNN model outperformed the multilinear regression model in solar radiation forecasting for the Northern Greece region [69].

Researchers have frequently compared ANN models and machine learning techniques in their studies on solar radiation forecasting. An ANN was developed to estimate the hourly values of three components of solar radiation (Horizontal Global, Horizontal Diffuse, and Normal Beam) in the Odeillo region of France. The prediction performance of this neural network model was compared with that of a RF model. During periods of high meteorological variability, the RF model predicted better [70]. However, this is not always an accepted phenomenon. In an hourly solar radiation forecast for Morocco, the proposed ANN model outperformed the RF model [71]. In another study, the same researcher proposed the Levenberg marquardt BPNN technique to estimate daily solar irradiance for the Fez region of Morocco [72]. Another machine learning model, FL, was compared with feed-forward BPNN method to estimate monthly solar irradiance for Dhaka, Bangladesh. The findings demonstrated that the neural network model performed better, achieving an accuracy of 98.78%. The comparison of the forecasting performance of the two models is presented in Fig. 9 [8]. In another study, the results of the ANN method developed to predict daily solar radiation are compared with the performance of k-NN, SVM, and deep learning models. The k-NN model achieved the worst prediction performance, while the BPNN model achieved the best prediction performance [73].

One of the factors that affect the prediction performance of ANN models is the characteristics and number of input parameters. ANN models built using different input combinations are compared to forecast daily solar radiation for the Samsun region. The aim here is to determine the variables that can predict the best solar radiation. To improve the prediction performance, the solar irradiance value of the previous day was added to the input parameters [74].

4.3. Machine learning

Machine learning (ML), which is likened to human natural behavior, is a trending field in today's informatics world [75]. The goal of ML is to take data and perform self-learning. Many researchers are working in this area to achieve high accuracy in ML approaches [76].

Multivariate Adaptive Regression Spline (MARS) technique, which is one of the regression methods that can evaluate multiple dependent and independent variables together, has an easy-to-understand and interpretable feature among machine learning methods. The MARS model is proposed for hourly GHI forecasting in Hong Kong, China. The performance of 16 MARS models, developed with different combinations of input variables, is analyzed [77]. The ML model used by many authors in the literature is the SVM. Solar radiation is variable throughout the day, but this variability follows a certain pattern under consistent weather conditions. If the slope of the radiation gradient is calculated based on this pattern, the future radiation value can be easily predicted. The working principle of the SVM is based on this [78]. SVM-based approaches were developed to estimate daily solar radiation in Beijing, China, and the researchers observed the effect of surface fog and haze on solar radiation estimation. In addition to the input variables, the air quality index (AQI) parameter is also included. When the results were compared, the SVM model with AQI input parameter improved the performance of the model by reducing the RMSE from 0.114 to 0.102 [79]. In another study, SVM models were considered depending on the input parameter. These models used certain meteorological factors as input and only relied on solar radiation data. For the first model, the SVM approach showed the best prediction performance with an R^2 value of 0.99 [80]. In addition to meteorological variables, cloud and sky images can also be used as input data. The forecasting performance of Gradient Boosting (GB) and k-NN techniques, developed to forecast hourly solar radiation in Folsom, California, is compared. The GB model performed more effectively with the addition of sky images to the input parameters [81]. The number and characteristics of the input parameters have an important impact on the efficiency of the SVM method, and optimizing these parameters can also affect the prediction accuracy. The proposed SVM-based method for daily solar irradiance forecasting in Beijing, China were optimized using Particle Swarm (PSO), Bat (BAT), and Whale (WOA) algorithms. It has been shown that heuristic algorithms

greatly improve the prediction performance of SVM [82].

Comparison of ML-based of techniques in the literature provide for to solar project investors and other researchers. In this way, it can provide ideas for selecting models for regions with similar climatic conditions. For example, a study was conducted to predict monthly solar radiation using five types of machine learning methods: Extreme Learning Machines (ELM), SVM, Gaussian Process Regression (GPR), k-NN, and LSTM method. The study utilized parameters from a total of 163 meteorological stations located in various climates across Turkey. It was observed that LSTM and GPR models are more effective for arid and semi-arid climates [83]. Twelve machine learning techniques were compared for forecasting monthly and daily solar radiation in Ganzhou, China. In Fig. 10, the error values and scatter plots of the machine learning models used to predict the monthly average solar radiation are displayed. GB technique demonstrated successful prediction performance in daily irradiance prediction, while XGBoost technique showed successful prediction performance in monthly irradiance prediction [84]. In another study, forty-five machine learning techniques were compared for forecasting monthly solar irradiance in Eskisehir, Turkey. According to the metric results, the best seven models were obtained as RF, Extra Trees, HistGB, Decision Tree (DT), Bagging Tree, LightGBM [85].

By approaching solar forecasting from a different direction, researchers have also emphasized the studies on estimating the energy obtained from the sun in power plants because solar irradiance value is the most important parameter in solar power estimation. Lasso Regression, k-NN, SVM models are compared in solar power estimation using solar irradiance data of Nigde, Turkey region. With an R^2 value of 0.997, SVM algorithm showed the best performance [86]. In another study, SVM, Linear Regression (LR), GPR, DT, and Community Regression (CR) models developed for short-term prediction of the energy obtained from the solar energy center in Australia were compared with each other. The SVM approach was found to provide the best prediction performance result [87]. In solar power forecasting studies, optimization of models improves the forecasting performance. The SVM model developed for power forecasting using solar radiation and temperature values for Victoria, Australia was optimized with GA. Thanks to the optimization, the SVM model RMSE value decreased from 680.85 to 11.226 and the prediction performance was improved [88].

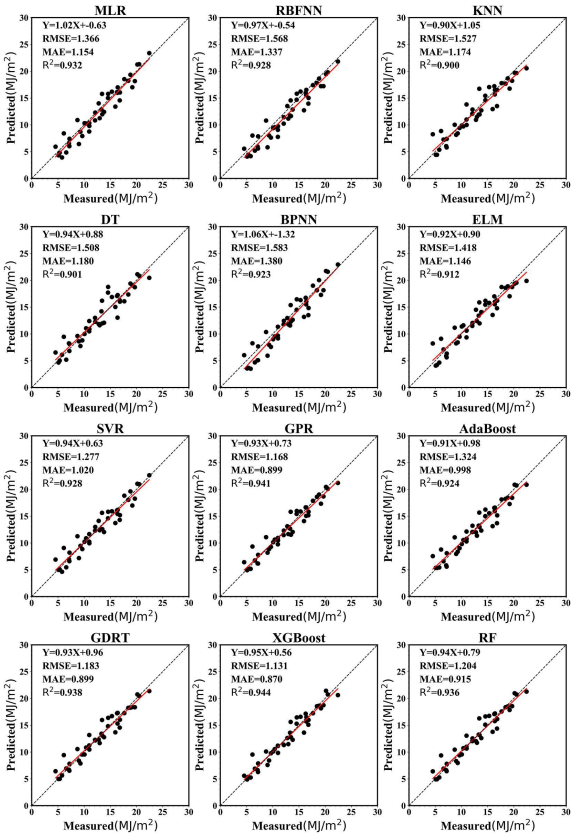

Fig. 10: Scatter plots of the results of machine learning models in predicting monthly average solar radiation [84].

4.4. Deep learning

Deep learning (DL), also known as hierarchical learning, is a specific area of ML and ANN with multiple hidden layers [89]. It is a phenomenon that enables computers to learn on their own from raw data without human intervention [90]. LSTM, Recurrent Neural Network (RNN), Deep Recurrent Neural Network (DRNN), and Convolutional Neural Network (CNN) are some of the deep neural network models [91]. The LSTM model is the most preferred method by researchers in the literature. A simple LSTM architecture has three parts: input, forget, and output gates. While the forget gate determines whether to retain or discard information, the input gate updates the information and transfers it to the output gate [92].

The LSTM architecture shown in Fig. 11 consists of repeating blocks: forget gate (f_t), input gate (i_t), and output gate (o_t). The process of detecting the information to be deleted using the input data $\mathbf{x_t}$ and $\mathbf{h_{t-1}}$ is given in Eq. (8). Here, the activation function is generally determined as sigmoid (σ).

$$ft = \partial(Wf, x^*Xt + Wf, h^*ht - 1 + bf) \qquad (8)$$

Eq. (9) and Eq. (10) are then used to determine new information in the input layer. After updating the

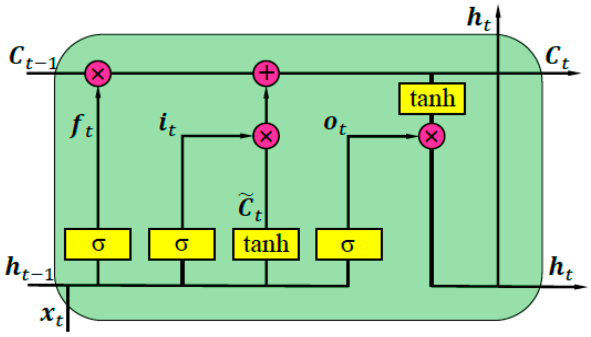

Fig. 11: Long Short-Term Memory Architecture [93].

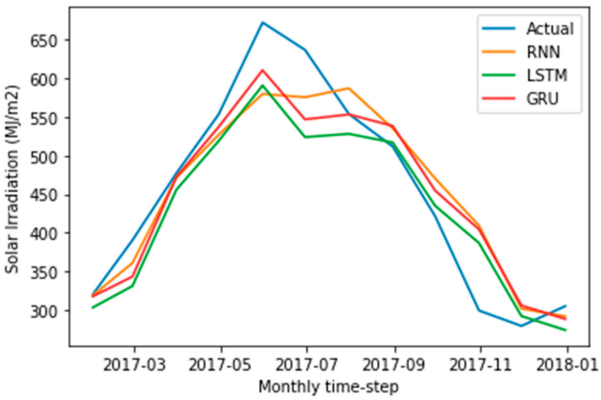

Fig. 12: Comparison graph of GRU, LSTM and RNN in monthly [101].

information with the sigmoid function, the candidate information that will contribute to forming the new information is identified using the tanh function.

$$it = \partial(Wi, x^*Xt + Wi, h^*ht - 1 + bi) \tag{9}$$

$$\overline{ct} = \tanh(Wc, x^*Xt + Wc, h^*ht - 1 + bc) \tag{10}$$

New information is generated using Eq. (11). Finally, in the output layer, Eq. (12) and Eq. (13) are used to obtain the output data. This process continues until the difference between the training values and the LSTM output values decreases. Weight parameters (W) and threshold values (b) are updated accordingly [93].

$$ct = ct - 1^*ft + ii^*\overline{ct} \tag{11}$$

$$ot = \sigma(Wo, x^*Xt + Wo, h^*ht - 1 + b0) \tag{12}$$

$$ht = ot^* \tanh(ct) \tag{13}$$

In order to address the issues of gradient fading and bursting during the training phase of the RNN model, researchers developed the LSTM architecture with memory cells and gate mechanism, as well as the Gated Recurrent Units (GRU) architecture [94].

Solar radiation estimation can be conducted for solar panels on ships as well as in desert areas, which are characterized by arid conditions. A researcher developed an LSTM model for estimating hourly solar irradiance in the Bikaner region of the Thar desert. The proposed model achieved the lowest RMSE value of 0.0995 for different time intervals [95]. Another study was conducted to forecast different time intervals for the city of Folsom, California. ANN and LSTM models were compared for predicting solar radiation at 1, 15, and 60-minute intervals. The LSTM model achieved better prediction results than the ANN model, with a MAPE value that was 1.63% lower. It is observed that the gap in prediction performance between the models narrows as the forecast horizon increases [96]. One study compares the ANN model for hourly solar irradiance forecasting in Santiago, Cape Verde. The performance of the BP Algorithm method and the proposed LSTM model are compared. When one year of data was used, the LSTM model achieved an accuracy of 18.34%. However, when 10 years of data was used, it achieved an accuracy that was 42.9% higher than the ANN model [97]. In the hourly solar radiation forecasting for South Korea, the proposed LSTM model outperformed the feed-forward neural network model [98].

RNN-based models suffer from a gradient problem when making long-term forecasts. In this study comparing RNN and LSTM models, they estimate GHI on an hourly and daily basis. The clarity index parameter is added as an input to enhance the forecast performance on cloudy days. Due to the memory issue in the RNN model, it was not able to perform as effectively as LSTM [99]. In order to address the memory issue in the RNN architecture, the Door Iterative Units (DIU) model has been developed and is used in comparative studies alongside LSTM models. GRU and LSTM models are compared in hourly solar radiation forecasting for Phoenix, Arizona. The LSTM model predicts with less error. In addition, GRU and LSTM models were found to give better results than univariate statistical models [100]. In another GRU-LSTM comparison study, the GRU model showed higher accuracy in hourly and daily solar radiation forecasting for Buson, Korea. Since GRU has two gates, the model complexity is lower than that of the LSTM model. This results in slightly better prediction performance of GRU, as shown in Fig. 12 [101]. LSTM architecture is also divided into different types. A study was conducted on time series models based on deep learning methodology for a region in India. LSTM, Bidirectional LSTM, GRU, Attention LSTM models have been developed for daily solar irradiance estimating. Here, the time series are based on single location univariate solar irradiance data as well as models that consider information from multiple locations [102].

Comparison studies of DL and ML methods are widely available in the literature. Three traditional ML models and three DL models (RF, SVM, Polynomial Regression, CNN, ANN, RNN) were compared in solar radiation prediction for Borno, Nigeria. In contrast to DL models, the RF model, which is one of the ML techniques, showed better prediction performance [103]. In contrast to the result mentioned here, the LSTM model improved the prediction performance for hourly solar radiation at Penn State by 71.5% compared to traditional ML methods [104]. In another daily solar radiation forecasting study for Çorum province, RF, k-NN, GB and DT models were compared with LSTM model. While the LSTM model gave the best result, the DT model showed the worst performance [105]. GB model, which is a derivative of DT, was compared with the LSTM model in a study on solar radiation forecasting in India. According to the metric results, the LSTM model showed prediction performance with less error. It is noteworthy that the estimation performance of the model changes according to the number of input variables. The LSTM model, which takes into account the meteorological information of the immediate region, obtained more accurate results than the LSTM model based only on past irradiance values [106]. The parameters and input variables of the LSTM model also affect the forecast performance. The forecasting capability of the LSTM method developed for hourly solar radiation forecasting in Denver, the capital city of Colorado, USA, was analyzed using different parameters. The model that takes into account the weather information for the next day has shown better performance [107].

5. Hybrid models

Researchers working on solar forecasting have developed hybrid models to achieve precise and highly accurate forecasts, which have become the preferred methods due to their ability to analyze data [108]. Since a dataset exhibits both linear and non-linear characteristics, utilizing a hybrid model instead of a single prediction model enhances performance. Hybrid models are used in three type ways: linear, non-linear, and both non-linear and linear [15].

Hybrid modeling is used enhance improve the performance of the ARIMA employed used in univariate time series forecasting modeling. This is achieved by extracting specific attribute values from historical data. The ARIMA model, which performs univariate time series analysis to forecast daily solar irradiance for the region of Morocco, was developed as a hybrid with an artificial neural network model [109]. In another study by the same author, the ARIMA model was used in combination with a feed-forward BP method for forecasting daily solar irradiance over the Moroccan region [56]. ANFIS are a type of ANN that combines the advantages of ANN and FL methods to create a powerful inference system. The proposed ANFIS model for forecasting monthly solar radiation over Malaysia is optimized using differential evolution (DE) algorithms, GA, PSO. Comparing the metric results, the ANFIS-PSO hybrid method achieved better prediction performance [110]. Comparison of actual measured data and ANFIS-PSO predicted data is shown in Fig. 13.

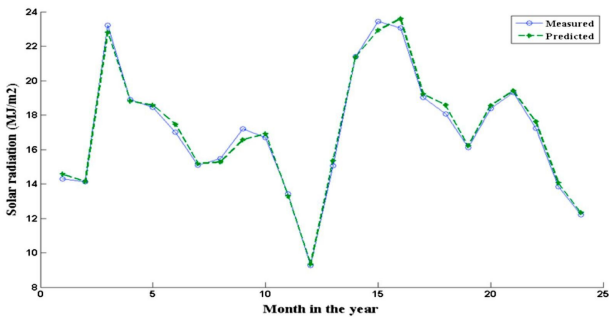

Fig. 13: Comparison actual measured data and ANFIS-PSO predicted data [110].

The another study aimed to minimize the prediction error of solar radiation by examining SVM models built in a hybrid way with optimization algorithms such as PSO and GA to obtain appropriate parameters [111]. Another type of ANN, known as the Multilayer Perceptron (MLP), is used in combination with CNN for short-term solar radiation prediction. The CNN method extracts features from sky images, and the MLP network utilizes this information to establish a correlation between solar irradiance and weather conditions [112]. In another study, hourly solar radiation forecasting was performed using a hybrid CNN model that incorporated satellite imagery. Here, the impact of cloud locations on the performance of solar irradiance estimating was investigated [113]. A hybrid model that utilizes satellite images and sky images was proposed for forecasting hourly solar radiation in France [114].

In the literature, DL-based hybrid models are among the most preferred methods for solar radiation forecasting. A LSTM-CNN hybrid model is proposed for forecasting hourly solar radiation in San Diego, California. The developed model yielded the best result for short-term solar radiation estimating under various weather conditions [115]. In contrast to this result, the LSTM-CNN model developed for daily solar radiation forecasting in an Australian solar farm did not perform as well as the proposed hybrid deep SCLC model [116].

The GRU model, which is simpler than the LSTM model, has certain advantages due to lower low parameterization faster high training speed. A hybrid

GRU-Attention model was proposed for short-term solar radiation forecasting for the Las Vegas region [117]. However, there are studies in the literature that indicate that single models demonstrate better prediction performance. ARIMA and Bidirectional Gated Unit (Bi-GRU) methods are combined for short-term solar irradiance estimating in South Korea. The developed hybrid method exhibits lower forecast performance compared to the individual models. This result challenges the notion that hybrid methods will always outperform single models in forecasting performance [118].

6. Results

This section, the formulas for the evaluation metrics are presented first. Subsequently, an example study predicting solar radiation using the ANFIS model is conducted. The performance evaluation results of the methods and approaches used for solar irradiance prediction in the literature are summarized in Tab. 3-10. Some limitations and potential drawback that should be considered in the review study are identified. Finally, the problems that need to be addressed and the solutions used in the literature are discussed.

Performance evaluation is a statistical metric used to measure the accuracy of models [92]. The accuracy criterion is crucial when evaluating the performance of forecasting techniques [73]. The error metrics commonly used in solar radiation forecasting models are as follows. In the equations, $Y_{(exp,i)}$ represents the actual value at time step i, $Y_{(forecast,i)}$ represents the observed value at time step i, μ represents the average of the actual value and N represents the number of data points to be evaluated.

Mean Bias Error shows the difference between of predicted values and their corresponding actual values. MBE is more effective in measuring long-term forecasting performance. A low MBE score indicates that the long-term forecasting model is functioning well [119].

$$MBE = \frac{1}{N}\sum_{i=1}^{N}(Y\exp,i - Yforecast,i) \tag{14}$$

Mean Absolute Error (MAE) is the average of the absolute differences between predicted and actual values in the dataset. A low MAE value indicates strong prediction performance [120].

$$MAE = \frac{1}{N}\sum_{i=1}^{N}|Yforecast,i - Y\exp,i| \tag{15}$$

MSE is the average of the squared differences difference between the actual and the predicted values.

Tab. 2: According to the prediction horizon, selecting a model that demonstrates superior performance.

Very-short term	Short-term	Medium-term	Long-term
Image-based	ML	ML	ML
Hybrids	DL	DL	DL
Hybrids	ARIMA	ARIMA	ANN

The square root of MSE is the Root Mean Square Error (RMSE). RMSE is an effective evaluation tool in short-term solar radiation forecasting. As the RMSE value approaches zero, the model's performance improves [121].

$$MSE = \frac{1}{N}\sum_{i=1}^{N}(Yforecast,i - Y\exp,i)^2 \tag{16}$$

$$RMSE = \sqrt{\frac{\sum_{i=1}^{N}(Yforecast,i - Y\exp,i)^2}{N}} \tag{17}$$

Coefficient of Determination (R^2 score) is a measure of how well the predictions approximate the true values. It indicates the linear relationship between the true and predicted values in the dataset. The R^2 score ranges between zero and one, and closer to one indicates better model performance [122].

$$R^2 = 1 - \frac{\sum_{i=1}^{N}(Y\exp,i - Yforecast,i)^2}{\sum_{i=1}^{N}(Y\exp,i - \mu)^2} \tag{18}$$

Example of solar irradiance predict:

Under this heading, the dataset used in the short-term forecasting of Global Horizontal Irradiance (GHI) with the ANFIS model and the results of the model's performance evaluation are presented. The dataset named "Renewable Energy and Weather Conditions" from the Kaggle data sharing site is utilized for short-term solar radiation forecasting with an ANFIS model. This dataset includes hourly meteorological information and energy consumption data from 2017 to 2022. The time-dependent graph displaying hourly solar irradiance information is presented in Fig. 14.

Energy exchange value (Wh), temperature, sunshine duration, and time of day were used as input parameters. For GHI estimation, 70% of the dataset is allocated to training data, while 30% is allocated to test data. The ANFIS model was created using the ANFIS Toolbax interface in MATLAB R2021a. The parameters of the ANFIS model are provided in Tab. 11.

The prediction performance of the ANFIS model is evaluated using RMSE and R^2 score metrics. The results of the prediction and training datasets are pre-

Tab. 3: According to the prediction horizon, selecting a model that demonstrates superior performance.

Name of model	Time horizon	Location	Forecast variable	MAE (W/m^2)	MBE (W/m^2)	RMSE (W/m^2)	rRmse (W/m^2)	R^2
MSG-SEVIRI	15 min	Netherland	GHI DHI	-	-	96	34	-
FY-4A(CSD-SI)	60 min	Northwest China	GHI	44.87	9.84	60.89	18.93	-
FY-4A(AGRI)	30 min	Chengde, China	DNI	148.43	5.31	240.01	40.96	-
GOES-H2	Daily	Saint Georges, France						
RTP-H2				-	70.0	106.4		0.94

Tab. 4: Performance of ground-based sky imager on solar irradiance forecasting.

Name of model	Time horizon	Location	Forecast variable	MAE (W/m^2)	MBE (W/m^2)	RMSE (W/m^2)	R^2
ASI-16	10 min	Golden, Colorado	GHI	15.61	-	16.02	-
ASI-Real Time Irradiance	1 min	Salto, Uruguay	GHI	112	25.5	184	-
Image based - Cloud Motion Tracking	5 min	Wollongong, Australia	GHI	13	-	18	-
ASI-16	Hourly	Taiwan	GHI	34.03	-	53.99	0.95
All Sky Imager-1	10 min	Spain	GHI	36.7	3.6	-	0.92
ASI-Cuboid	10 min	Golden, Colorado	GHI	-	-	67.57	-
DenseNet-121	10 min	Golden, Colorado	GHI	49.1	-	80.4	-
ASI-kNN	Hourly	Golden, Colorado	GHI	-	-	116.7	-
Sky Image Irradiance Mapping - SVM	Hourly	Wasco Power Station	GHI	-	-	92.72	-

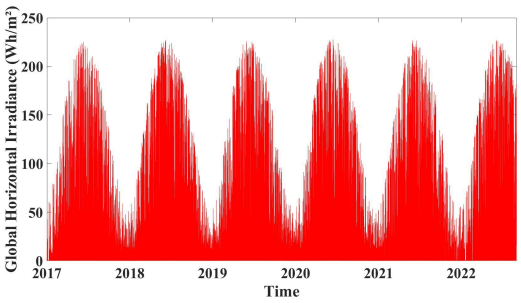

Fig. 14: Global Horizontal Irradiance value between 2017-2022.

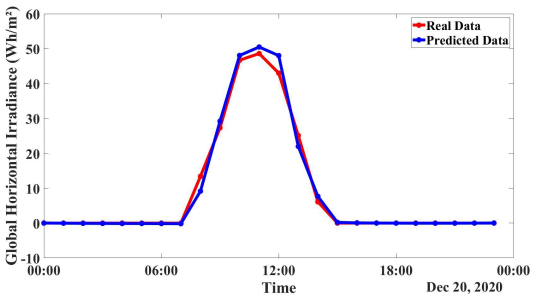

Fig. 15: The forecasted results of GHI with Dec 20, 2022.

sented in Tab. 12. The daily solar radiation forecasting graphs selected from months representing the four seasons from the test data are shown in Fig. 15-21. The RMSE and R^2 evaluation of the forecast results for the specified days are presented in Tab. 13.

In selecting a forecasting model, it is essential to consider the relationship between the forecasting horizon and the model's performance to determine the universally best approach. Upon examining the results tables, methods yielding low error and high R^2 values are classified in Tab. 2. This study demonstrates that machine learning and deep learning methods exhibit high accuracy in forecasting performance across all forecasting horizons. While image-based methods perform effectively for very short-term forecasting, ARIMA-based models show strong performance for long- and medium-term forecasts. Hybrid approaches achieve high accuracy in short-term horizons, whereas ANN methods are observed to be effective for medium-term horizons. In solar irradiance studies, the relationship between the forecasting horizon and model selection is previously indicated in Tab. 1. The findings suggest that the superiority of a forecasting model is determined by the chosen model relative to the forecasting horizon rather than meteorological and geographical conditions.

Although hybrid models exhibit high accuracy in forecasting performance, their complex structures can pose challenges in the prediction process. Optimization algorithms are employed to mitigate this complexity and cost [123]. Data preprocessing, outlier detection, and feature extraction reduce the computational steps in prediction calculations. In solar irradiance forecasting for the Saudi Arabian region, four different algorithms were used to select distinct features. The results showed that feature selection significantly reduced computational costs by eliminating unnecessary information and achieved good forecasting performance. In another study utilizing feature extraction and dimensionality reduction techniques, the model complexity

Tab. 5: Performance of numerical weather prediction on solar irradiance forecasting.

Name of model	Time horizon	Location	Forecast variable	MAE (W/m^2)	MBE (W/m^2)	RMSE (W/m^2)	FS
FARMS-DNI	Hourly	Southern	DNI	151.76	-	203.59	-
WRF	Hourly	Gifu, Japan	GHI	-	96	210	-
WRF-Solar-PCA	Hourly	Singapore	GHI	133	-14	169	-
MLP – NWP Post Process	Monthly	Pennsylvania	GHI	91.1 (NMAE)	6.3 (NMBE)	-	-
ECMWF-HRES	Hourly	Desert Rock	GHI	44	-9	74	-
ACCESS	Daily	Australia	GHI	-	-	-	0.26
GFS HRRR-Kalman Filter	Hourly	Goodwin Creek, Mississippi	GHI	-	0.31	-	-

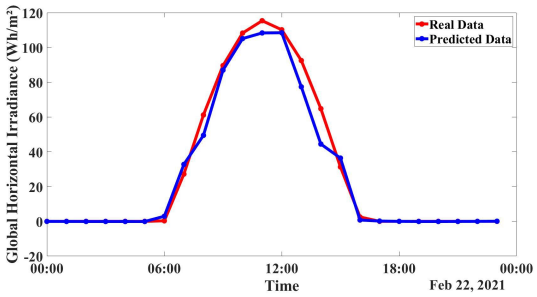

Fig. 16: The forecasted results of GHI with Feb 22, 1022.

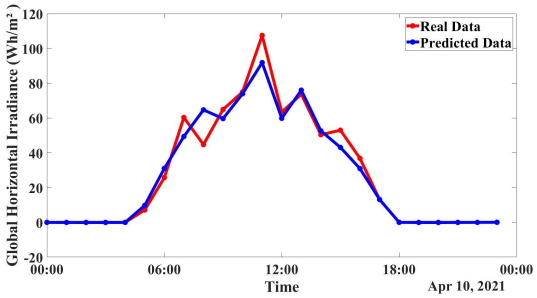

Fig. 17: The forecasted results of GHI with Apr 10, 2021.

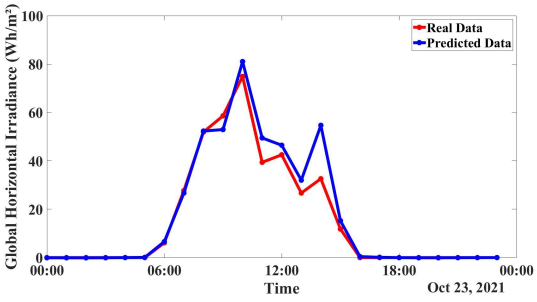

Fig. 18: The forecasted results of GHI with Oct 23, 2021.

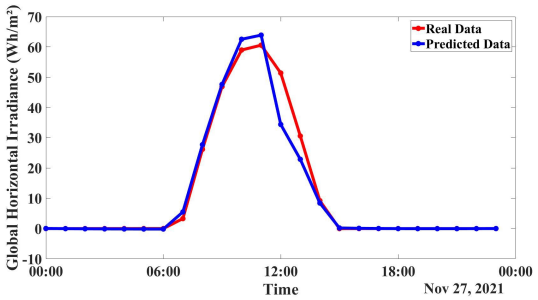

Fig. 19: The forecasted results of GHI with Nov 27, 2021.

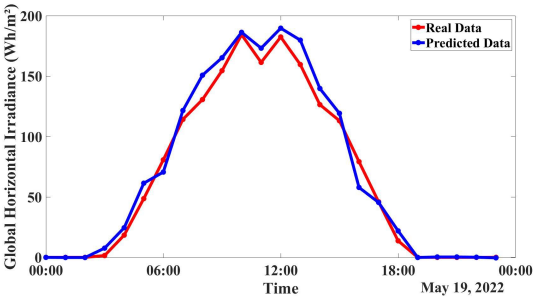

Fig. 20: The forecasted results of GHI with May 19, 2022.

was reduced, leading to solar forecasts with smaller error values [124].

Despite promising advancements in solar forecasting, artificial intelligence (AI), and deep learning methods face significant barriers in terms of transparency and explainability. This lack of transparency can lead to distrust in the adoption of AI models. Therefore, enhancing the transparency and explainability of AI-based models is a priority. Establishing rules for model decisions, using techniques like Local Interpretable Model-agnostic Explanations (LIME) and Shapley Additive Explanations (SHAP), and visualizing the model structure clarify the prediction process. In a solar forecasting study conducted in Bangladesh, incorporating explainable AI approaches such as SHAP, LIME, and Explain Like I'm 5 (ELI5) resulted in a secure and sustainable energy solution [125]. Another solar forecasting study in Fez, Morocco, used Permutation Feature Importance (PFI) and SHAP interpretation techniques

Tab. 6: Performance of ARIMA on solar irradiance forecasting.

Name of model	Input variables	Time horizon	Location	Forecast variable	MAE (W/m^2)	MBE (W/m^2)	RMSE (W/m^2)	R^2
ARIMA $(1,0,1)\times(0,1,1)_{12}$	Montlhy GHI values between 1984-2015	Monthly	Delhi, India	GHI	0.28 (kWh/m^2)	-	0.38 (kWh/m^2)	-
ARIMA $(4,0,1)\times(0,1,1)_{12}$	Monthly GHI values between 1984-2015	Monthly	Delhi, India	GHI	0.24 (kWh/m^2)	-	0.32 (kWh/m^2)	0.92
ARIMA $(0,0,1)\times(0,1,1)_{12}$	Hourly GHI values between 2005-2020	Monthly	Amman, Jordan	GHI	-	-	13.53	0.99
ARMA(3,3)	GHI values at 5 min intervals in 2010	Daily	North, Barcelona	GHI	0.2581	-	0.5414	-
SARIMA	Hourly GHI values between 2015-2020	Hourly	Missour, Morocco	GHI	-	-2.92	28.58	0.94
SARIMA $(1,1,2)\times(4,1,1)_{12}$	Hourly GHI values between 1981-2017	Monthly	Seul, South Korea	GHI	-	-	33.18	0.62
SARIMAX $(0,0,1,2)\times(0,0,0)_{12}$	Hourly GHI, DHI, DNI, etc. values between 2015-2019	Monthly	Islamabad, Pakistan	GHI	35.23	-	63.54	0.94
ARIMA (1,0,1)	From National Renewable Energy Laboratory	Hourly	Golden, Colorado	DHI	13.211	-	16.03	-
ARIMA (2,1,0)	GHI values at 10 minutes intervals in 2014- 2016	Monthly	Jaffna, Sri Lanka	DHI	-	-	29.644	-
ARIMA (2,2,1)	Hourly GHI values between 2013-2015	Hourly	Tetouan, Morocco	GHI	-	9.538	22.014	-
ARIMA (2,2,0)	Daily GHI values in 2015	Daily	Tangier, Morocco	GHI	-	0.0042 (kW/m^2)	0.60 (kWh/m^2)	0.97
ARIMA (0,2,1)	Daily GHI values between 2018-2019	Monthly	Tetouan, Morocco	GHI	-	0.45	1.35	-

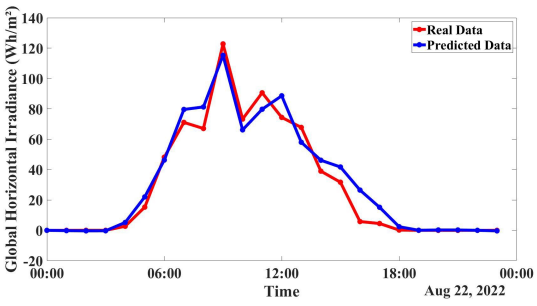

Fig. 21: The forecasted results of GHI with Aug 22, 2022.

to explain and improve machine learning model predictions. Independent interpretation techniques revealed how each parameter influenced the model's forecasts [126].

For a better understanding of AI-based models, they must be interpretable and explainable. A solar forecasting study in the Saudi Arabian region developed an explainable meta-heuristic-based fuzzy system. The model continuously updates itself to maintain interpretability through a lifelong learning process. The proposed method achieved 13.2% higher accuracy than other black-box models [127]. In Australia, a solar irradiance forecasting study developed an explainable AI model calibrated with uncertainty quantification. The explanations generated by the model provided users with insights into the impact of each variable. This enhances model stability and reliability for external stakeholders in the energy sector [128].

Privacy and ethical considerations are additional barriers to the adoption of AI-based models. Some AI technologies are being developed to process sensitive data while protecting individual privacy. In a study on solar energy, homomorphic encryption was used to perform computations while encrypting the data. This method outperformed models without privacy protection. Privacy protocols not only promote the ethical use of AI-based models but also enhance the model's forecasting ability [129].

The sustainability of ML-based models is a crucial measure of their ability to adapt to changing conditions. Additionally, some resource limitations, such as training time and processing speed, may arise in studies using large data sets. In a solar study conducted in

Tab. 7: Performance of ANN on solar irradiance forecasting.

Training Algorithm	Input variables	Time horizon	Location	Forecast variable	MAE (W/m^2)	MBE (W/m^2)	RMSE (W/m^2)	R^2
Elman BP	ATM, AT, RH, WS, etc.	Monthly	Chandigarh, India	GHI	0.026	-	-	0.99
Momentum and learning rate coefficients BP	GSR, Temp, RH, ATM	Daily	Aswan, Egyptia	GHI	-	-	1.55 (MJ/m^2)	0.99
Levenberg marquardt BP	Avg GSR, month/hour when estimation performed	Hourly	Surabaya, Indonesia	GHI	-	-	-	0.98
Levenberg marquardt BP	AT, WS, RH, sunshine duration, cloud cover	Daily	Mersin, Turkey	GHI	-	0.18 (kWh/m^2)	1.10 (kWh/m^2)	0.75
Levenberg marquardt BP	AT, RH, WS, ATM, etc.	Monthly	Antakya, Turkey	GHI	-	-	0.28 (MJ/m^2)	0.99
BP	AT, RH, GSR, WS	Daily	Northern, Greece	GHI	-	-	3.16 (MJ/m^2)	0.88
Levenberg marquardt BP	GSR, DHI, BHI	Daily	Odeillo, France	GHI	72.87	-	101.79	-
				BNI	168.14	-	212.33	-
				DHI	40.61	-	56.77	-
Levenberg marquardt BP	RH, Temp, GSR	Daily	Fez, Morocco	GHI	-	-	-	0.97
BP	Temp, RH, ATM, WS	Monthly	Dhaka, Bengladesh	GHI	-	-	0.31 (kWh/m^2)	0.99
BP	Temp, cloud cover, GSR	Daily	Nevsehir, Turkey	GHI	-	0.195 (MJ/m^2)	2.157 (MJ/m^2)	0.93
Levenberg marquardt BP	GSR, Temp, WS, RH, etc.	Daily	Samsun, Turkey	GHI	-	-	0.577	0.96

*ATM: Atmospheric Pressure, *AT: Air Temperature, *Temp: Temperature, *RH: Relative Humudity, *WS: Wind Speed, *Avg: Average, *GSR: Global Solar Radiation, *BHI: Beam Horizontal Irradiance

China, a radiative transfer learning approach achieved high-speed and high-accuracy forecasts with fewer resources compared to complex and multi-layered models [130]. Another advantage of the transfer learning approach is its ability to improve GHI forecasting performance by transferring valuable parameter information when data availability is insufficient [131]. Incremental learning ensures that learned knowledge can be applied to new data without being forgotten, thus facilitating the model's adaptation to changing conditions. In a solar study utilizing an incremental learning algorithm, the proposed model readily adapted to climate changes [132].

The assumption that long forecast horizons have low predictability and clear skies have high predictability is quite common in the literature. However, a study challenging these traditional assumptions created predictability maps. It demonstrated that the predictability of the atmospheric process could be determined by an equation that considers the performance of a series of forecasts and a reference set. The results showed that predictability is not dependent on the forecast horizon or climate and sky cloud conditions [133]. High-accuracy forecasts can be achieved by adjusting the parameter values of the model for regions with different meteorological conditions [11].

In regions where meteorological data are not secure, forecasting performance is directly affected. For areas where data measurement is not possible or sufficient, climate simulations obtained from Global Climate Models (GCMs) are used. GCMs provide an efficient and sustainable means of utilizing solar energy [134]. The increase in climate change limits the reliability of meteorological data due to environmental factors. In Nigeria, a solar study was conducted under different climate scenarios resulting from the effects of global warming. The use of GCM outputs allowed for a better assessment of the impact of climate change and the quality of meteorological data [135].

7. Conclusion

Solar energy stands out as one of the most favored renewable energy sources due to its cleanliness, cost-effectiveness, and sustainability. However, its intermittent nature and variable power output necessitate accurate irradiance estimation for feasibility studies in the energy sector. Over the past five years, significant research has been conducted in this field, as evidenced by literature reviewed in this article. Additionally, an application using the ANFIS model for solar radiation estimation is presented, which serves as a practical example for newcomers to this field. Notably, the ANFIS model achieved the most accurate solar forecast with an RMSE of 1.641 and an R^2 value of 0.996 for Decem-

Tab. 8: Performance of machine learning on solar irradiance forecasting.

Name of model	Input variables	Time horizon	Location	Forecast variable	MAE (W/m^2)	MBE (W/m^2)	RMSE (W/m^2)	R^2
MARS	GHI, sunshine duration, visibility, cloud cover amount, WS	Hourly	Hong Kong, China	GHI	0.198 (MJ/m^2)	-0.021 (MJ/m^2)	0.274 (MJ/m^2)	0.91
SVM	GHI, Temp, RH, sunshine duration, AQI	Daily	Beijing, China	GHI	-	-	0.076 (MJ/m^2)	0.95
SVM	Temp, ATM, RH, WS and local timeshine duration, AQI	Hourly	Abu Musa Island	GHI	-	-	3.026	0.95
GB	GHI, DNI, sky images	Minutely	Folsom, California	GHI	-	-	34.4	-
				DNI	-	-	71.3	-
SVM-PSO	GHI, DHI, sunshine duration, Temp, air pollutans	Daily	Beijing, China	GHI	0.741 (MJ/m^2)	-	-	0.92
GPR	GHI, Temp, WS, Lon, Lat, RH	Monthly	163 Met. Stat. in Turkey	GHI	-	-	-	0.87
GBRT	Temp, precipitation, ATM, RH, WS, visibility, sunshine duration	Daily	Ganzhou, China	GHI	1.498 (MJ/m^2)	-	1.987 (MJ/m^2)	0.92
XGBoost		Monthly			0.870 (MJ/m^2)	-	1.131 (MJ/m^2)	-
Extra Trees	Sky insolation, RH, precipitation, ATM, radiation flux, Temp, WS, sky clearness	Monthly	Eskisehir, Turkey	GHI	5.67	-	8.05	0.99
kNN	Temp, GSR	Monthly	Nigde, Turkey	Solar Power	0.045 (kW)	-	0.067 (kW)	0.99
SVM	Power, Temp, RH, GSR	Hourly	Alice Springs, Australia	Solar Power	0.015 (kW)	-	0.024 (kW)	0.99
SVM-GA	Temp, GSR	Hourly	Victoria, Australia	Solar Power	-	-	11.226 (W)	-

*ATM: Atmospheric Pressure, *Temp: Temperature, *RH: Relative Humudity, *WS: Wind Speed, *GSR: Global Solar Radiation,
*Lon: Longitude, *Lat: Latitude, *AQI: Air Quality Index, *Met. Stat: Meteorology Station

ber 20, 2020. The prediction performance and model findings of the models in the literature, classified according to methods, are summarized in Tab. 3-10.

Solar radiation forecasting methods can be categorized based on the method and forecast horizon, including very short-term, short-term, medium-term and long-term predictions. Models utilizing sky and satellite imagery demonstrate high accuracy for very short-term forecasting under various weather conditions. For satellite image-based models, RMSE values range from 60.89 W/m^2 to 346 W/m^2, while the MAE values vary from 45.26 W/m^2 to 224.51 W/m^2. Ground-based sky imager models achieve RMSE values ranging from 18 W/m^2 to 251 W/m^2 with R^2 values between 0.89 and 0.98. The performance of these models is directly influenced by cloud properties such as movement, speed, and thickness.

NWP models are utilized for short and medium-term forecasts, with MAE values ranging from 44 W/m^2 to 151.76 W/m^2 and RMSE values from 74 W/m^2 to 203.59 W/m^2. Various statistical techniques are employed for forecasting across different time horizons. ARIMA-based models are frequently utilized for analyzing time series data in solar radiation forecasting. These models address the seasonal nature of solar radiation by capturing seasonal patterns and trends. In addition to ARIMA, SARIMA models incorporate seasonality into the forecasting process. SARIMAX models extend SARIMA by incorporating exogenous variables, allowing for the inclusion of additional predictors that may influence solar radiation levels. RMSE values of ARIMA-based models range from 0.5414 W/m^2 to 63.54 W/m^2, while the MAE values range from 0.2581 W/m^2 to 35.23 W/m^2. The prediction performance is achieved the highest R^2 value of 0.99.

Tab. 9: Performance of hybrids on solar irradiance forecasting.

Name of model	Input variables	Time horizon	Location	Forecast variable	MAE (W/m^2)	MBE (W/m^2)	RMSE (W/m^2)	R^2
ARIMA-ANN	GSR	Daily	Tanger, Morocco	GHI	-	-3.430	446.35	0.98
ARIMA-FFBP	Ambient temperature, WS, RH, Lat etc.	Daily	Tanger, Morocco	GHI	-	0.022 (kWh/m^2)	0.307 (kWh/m^2)	0.99
ANFIS-PSO	Sunshine duration and AT	Monthly	Kuala Terengganu, Malaysia	GHI	-	-	0.306 (MJ/m^2)	0.99
CNN-MLP	Hemispheric camera images, GSR, Temp, RH, WS,WD	Daily (Cloudy)	Benguerir, Morocco	GHI	-	-7.66	49.16	0.94
		Daily (Clear)		GHI	-	-0.87	13.05	0.99
Satellite images + CNN	Temp, RW, ATM, WS, RF, cloud factors, past irradiance values, solar zenith angle, satellite images	Hourly (Winter)	Shandog, China	GHI	15.7	-	22.2	-
		Hourly (Summer)			25.7	-	31.6	-
Satellite images + Sky images	Sky images, satellite observations, past GSR	Hourly	France	GHI	-	-	134.9	-
LSTM-CNN	Temp, WS, RH, precipitation, DP, cloud type, clear-sky irradiance value etc.	Hourly	San Diego, California	GHI	27.38	-	42.89	0.98
Deep Hybrid SCLC	GSR, WS, air quality	Daily	Barunggam, Australia	GHI	-	-	2.338 (MJ/m^2)	0.93
GRU-Attention	GSR, WS	30-min (Winter)	Nevada, Las Vegas	GHI	33.66	-	41.69	0.99
		30-min (Summer)			38.33	-	44.15	
Bi-GRU - ARIMA	GSR, Temp, RH, WS etc.	Minutely	Jinju, South Korea	GHI	34.16	-	72.28	0.93
		Hourly			77.63	-	104.4	0.84

*ATM: Atmospheric Pressure, *AT: Air Temperature, *Temp: Temperature, *RH: Relative Humudity, *WS: Wind Speed,
*WD: Wind Direction, *RF: Rainfall, *GSR: Global Solar Radiation, *DP: Dew Point, *Lat: Latitude

Among the individual models utilized in the literature, artificial intelligence, machine learning, and deep learning techniques are predominantly employed. In these models, the lowest RMSE value recorded was 0.099 W/m^2, and the lowest MAE value was 0.026 W/m^2. The R^2 value ranges from 0.87 to 0.99. Researchers prefer using multiple models simultaneously or combining optimization algorithms to enhance parameters, rather than relying on a single method for higher accuracy. Hybrid models, the RMSE value ranges from 0.99 W/m^2 to 134.9 W/m^2. The highest R^2 value achieved is 0.99, with the lowest MAE value recorded at 15.7 W/m^2.

Most reviewed articles compare linear models with nonlinear models, deep learning models with traditional machine learning models, and hybrid models with single models. Other studies have focused on some potential limitations that need to be considered. To reduce the structural complexity and computational cost of hybrid models, optimization algorithms, data preprocessing, outlier detection, and feature extraction techniques have been applied. The interpretability of AI algorithms enhances the transparency and reliability of the models.

The selection of the forecasting region depends on its suitability for solar energy investments or places where direct solar measurements are not practical. Given the intermittency of solar energy, particularly in the winter months, some studies have concentrated on forecasting solar radiation during these periods. In situations

Tab. 10: Performance of deep learning on solar irradiance forecasting.

Name of model	Input variables	Time horizon	Location	Forecast variable	MAE (W/m^2)	MBE (W/m^2)	RMSE (W/m^2)	R^2
LSTM	DHI,DNI, DP, Temp, ATM, RH, WS, WD	Hourly	Bikaner, Thar Desert	GHI	-	-	0.099	-
LSTM	AT, WS, Precipitation, RH, ATM, GSR	Hourly	Folsom, California	GHI	-	-	-	0.86
LSTM	Temp, DP, RH, visibility, WS	Hourly	Cape Verde, Santiago	GHI	-	-	76.245	-
LSTM	Daily GSR, Cloud type, DP, Temp, RH, Solar zenith angle, WS	Hourly	Atlanta, New York	GHI	30.19	-	41.37	0.97
LSTM	Solar zenith angle, RH, ATM, GSR	Hourly	Phoenix, Arizona	GHI	-	-	66.75	-
GRU	Hourly and daily GSR	Hourly	Buson, Korea	GHI	-	-	0.458	-
LSTM	Daily GSR	Daily Daily	India	GHI	- -	-	6.316 3.166	- 0.88
CNN	Ambient temperature, WS, sun height, GSR, DHI	Hourly	Borno, Nigeria	GHI	37.87	-	83.44	0.95
RNN				DHI	20.00		52.65	0.89
LSTM	Daily GSR, clear sky GSR	Hourly	Penn State, United States	GHI	-	-	7.73	-
LSTM	Daily GSR	Daily	Corum, Turkey	GHI	15.87	-	20.34	0.75
LSTM	GSR of neighboring location, WD, WS	Hourly Daily	India	GHI	18.1 31.7	-	50.3 83.8	- -
LSTM	GSR, ambient temperature, RH, WS, ATM, precipitation	Hourly	Denver Colorado USA	GHI	-	-	75.22	-

*ATM: *ATM: Atmospheric Pressure, *Temp: Temperature, *RH: Relative Humudity, *WS: Wind Speed, *WD: Wind Direction, *GSR: Global Solar Radiation, *DP: Dew Point

Tab. 11: Relationship between forecasting horizon and forecasting method.

The parameters of the ANFIS model.	Value
MF type	Trim Function
Output MF	Linear
Number of nodes	193
Number of training data pairs	34440
Number of fuzzy rules	81

Tab. 12: The results of the prediction and training datasets.

ANFIS Model	RMSE(W/m^2)	R^2
Train	12.135	0.972
Test	13.964	0.965

where meteorological values cannot be measured or are inadequate, climate simulations are utilized.

This study presents summarized findings from various articles examining parameters such as predicted regions, forecasting periods, meteorological measurements, and model complexities. Additionally, it addresses potential limitations in the field of solar forecasting and summarizes solutions to these issues as discussed in the literature. This provides a comprehensive perspective on the field of solar forecasting and shapes future research directions.

Author Contributions

T.S encouraged F.Y to conduct research on the specified topic. F.Y and T.S developed and drafted the outline for the article. F.Y, compiled other original studies

Tab. 13: The forecast results of the specified days.

Predict Day	RMSE(W/m^2)	R^2
Dec 20, 2020	1.641	0.996
Feb 22, 2021	6.177	0.992
Apr 10, 2021	6.398	0.981
Oct 23, 2021	5.465	0.980
Nov 27, 2021	3.980	0.981
May 19, 2022	9.698	0.993
Aug 22, 2022	8.044	0.977

on the topic from the literature and categorized them based on their methods. F.Y analyzed the methods by presenting the results in a comparative manner. T.S provided critical feedback and assisted in the research, analysis, and development of the paper. F.Y took the lead in writing the paper. All authors discussed the results and contributed to the final manuscript.

References

[1] ZAMBRANO, A. F., L. F. GIRALDO. Solar irradiance forecasting models without on-site training measurements. *Renewable Energy*. 2020, vol. 152, pp. 557–566. DOI: 10.1016/J.RENENE.2020.01.092.

[2] GRIGORIOS, L. K.. Low carbon energy technologies in sustainable energy systems. *Academic Press*. 2021.

[3] MARTÍN, L., L. F. ZARZALEJO, J. POLO, A. A. NAVARRO, R. MARCHANTE, M. CONY. Prediction of global solar irradiance based on time series analysis: Application to solar thermal power plants energy production planning. *Solar Energy*. 2010, vol. 84, iss. 10, pp. 1772–1781. DOI: 10.1016/J.SOLENER.2010.07.002.

[4] RYABUSHEV, Y. A.. Solar energy as alternative energy source: advantages and disadvantages. 2022.

[5] STEVANOVIĆ, S., S. STEVANOVIĆ, R. ŽIVKOVIĆ. Advantages and disadvantages of solar energy production and use. *Journal of Agricultural and Food and Environmental Sciences*. 2022, vol. 76, no. 4. DOI: 10.55302/JAFES22764065s.

[6] ALZAHRANI, A., P. SHAMSI, C. H. DAGLI, M. FERDOWSI. Solar Irradiance Forecasting Using Deep Neural Networks. *Procedia Computer Science*. 2022, vol. 114, pp. 304–313. DOI: 10.1016/J.PROCS.2017.09.045.

[7] BELMAHDI, B., M. LOUZAZNI, A. EL BOUARDI. One month-ahead forecasting of mean daily global solar radiation using time series models. *Optik*. 2020, vol. 219. DOI: 10.1016/J.IJLEO.2020.165207.

[8] AHMED, Md. B., M. A. CHOWDHURY, S. AHMED, M. A. KASHEM. Prediction of solar irradiation and performance evaluation of grid connected solar 80KWp PV plant in Bangladesh. *Energy Reports*. 2019, vol. 5, pp. 714–722. DOI: 10.1016/J.EGYR.2019.06.011.

[9] ELLAHI, M., G. ABBAS, I. KHAN, P. M. KOOLA, M. NASIR, A. RAZA, U. FAROOQ. Recent Approaches of Forecasting and Optimal Economic Dispatch to Overcome Intermittency of Wind and Photovoltaic (PV) Systems: A Review. *Energies*. 2019, vol. 12, no. 22. DOI: 10.3390/EN12224392.

[10] KUMAR, D. S., G. M. YAGLI, M. KASHYAP, D. SRINIVASAN. Solar irradiance resource and forecasting: a comprehensive review. *IET Renewable Power Generation*. 2010, vol. 14, iss. 10, pp. 1641–1656. DOI: 10.1049/IET-RPG.2019.1227.

[11] CHODAKOWSKA, E., J. NAZARKO, Ł. NAZARKO, H. RABAYAH, R. ABENDEH, R. ALAWNEH. ARIMA Models in Solar Radiation Forecasting in Different Geographic Locations. *Energies*. 2023, vol. 16, no. 13. DOI: 10.3390/en16135029.

[12] NARVAEZ, G., L. F. GIRALDO, M. BRESSAN, A. PANTOJA. Machine learning for site-adaptation and solar radiation forecasting. *Energies*. 2021, vol. 167, pp. 333–342. DOI: 10.1016/J.RENENE.2020.11.089.

[13] INMAN, R. H., H. T.C PEDRO, C. F.M. COIMBRA. Solar forecasting methods for renewable energy integration. *Progress in Energy and Combustion Science*. 2013, vol. 39, iss. 6, pp. 535–576. DOI: 10.1016/J.PECS.2013.06.002.

[14] MISHRA, M., P. MAHAJAN, R. GARG. Comparison and Analysis of Solar Irradiance Forecasting Techniques. *2022 IEEE Delhi Section Conference (DELCON), New Delhi, India*. 2022. DOI: 10.1109/DELCON54057.2022.9753206.

[15] DIAGNE, M., M. DAVID, P. LAURET, J. BOLAND, N. SCHMUTZ. Review of solar irradiance forecasting methods and a proposition for small-scale insular grids. *Renewable and Sustainable Energy Reviews*. 2013, vol. 27, pp. 65–76. DOI: 10.1016/J.RSER.2013.06.042.

[16] BOSCH, J.L., J. KLEISSL. Cloud motion vectors from a network of ground sensors in a solar power plant. *Solar Energy*. 2013, vol. 95, pp. 13–20. DOI: 10.1016/J.SOLENER.2013.05.027.

[17] KRISHNAN, N., K. R. KUMAR, C. S. INDA. How solar radiation forecasting impacts the utilization of solar energy: A critical review.

Journal of Cleaner Production. 2023, vol. 388. DOI: 10.1016/j.jclepro.2023.135860.

[18] WANG, P., R. V. WESTRHENEN, J. F. MEIRINK, S. V. D. VEEN, W. H. KNAP. Surface solar radiation forecasts by advecting cloud physical properties derived from Meteosat Second Generation observations. *Solar Energy*. 2019, vol. 177. DOI: 10.1016/J.SOLENER.2018.10.073.

[19] YANG, L., X. GAO, Z. LI, D. JIA, J. JIANG. Nowcasting of Surface Solar Irradiance Using FengYun-4 Satellite Observations over China. *Remote Sens.* 2019, vol. 11, no. 17. DOI: 10.3390/RS11171984.

[20] YANG, L., X. GAO, J. HUA, P. WU, Z. LI, D. JIA. Very Short-Term Surface Solar Irradiance Forecasting Based On FengYun-4 Geostationary Satellite. *Sensors*. 2020, vol. 20, no. 9. DOI: 10.3390/S20092606.

[21] MOUHAMET, D., A. TOMMY, A. PRIMEROSE, L. LAURENT. Improving the Heliosat-2 method for surface solar irradiation estimation under cloudy sky areas. *Solar Energy*. 2018, vol. 169, pp. 565–576. DOI: 10.1016/J.SOLENER.2018.05.032.

[22] WANG, F., et al. A minutely solar irradiance forecasting method based on real-time sky image-irradiance mapping model. *Energy Conversion and Management*. 2020, vol. 220. DOI: 10.1016/J.ENCONMAN.2020.113075.

[23] SCHMIDT, T., J. KALISCH, E. LORENZ, D. HEINEMANN. Evaluating the spatio-temporal performance of sky-imager-based solar irradiance analysis and forecasts. *Atmospheric Chemistry and Physics Discussions*. 2016, vol. 16. DOI: 10.5194/ACP-16-3399-2016.

[24] MANANDHAR, P., M. TEMIMI, Z. AUNG. Short-term solar radiation forecast using total sky imager via transfer learning. *Energy Reports*. 2023, vol. 9. DOI: 10.1016/j.egyr.2022.11.087.

[25] KURTZ, B., F. A. MEJIA, J. KLEISSL. A virtual sky imager testbed for solar energy forecasting. *Solar Energy*. 2017, vol. 158. DOI: 10.1016/J.SOLENER.2017.10.036.

[26] WU, X., et al. Multidimensional Feature Extraction Based Minutely Solar Irradiance Forecasting Method Using All-Sky Images. *IEEE Transactions on Industry Applications*. 2024, vol. 60, no. 3. DOI: 10.1109/tia.2024.3372515.

[27] CALDAS, M., R. ALONSO-SUÁREZ. Very short-term solar irradiance forecast using all-sky imaging and real-time irradiance measurements. *Renewable Energy*. 2019, vol. 143. DOI: 10.1016/J.RENENE.2019.05.069

[28] DISSAWA, L. H., et al. Sky Image-Based Localized, Short-Term Solar Irradiance Forecasting for Multiple PV Sites via Cloud Motion Tracking. *Renewable Energy*. 2021, vol. 2021. DOI: 10.1155/2021/9973010.

[29] CHU, T.-P., J. GUO, Y.-G. LEU, L.-F. CHOU. Estimation of solar irradiance and solar power based on all-sky images. *Solar Energy*. 2023, vol. 249. DOI: 10.1016/j.solener.2022.11.031.

[30] LOGOTHETIS, S.-A., et al. Benchmarking of solar irradiance nowcast performance derived from all-sky imagers. *Renewable Energy*. 2022, vol. 199. DOI: 10.1016/j.renene.2022.08.127.

[31] LIU, J., H. ZANG, T. DING, L. CHENG, Z. WEI, G. SUN. Harvesting spatiotemporal correlation from sky image sequence to improve ultra-short-term solar irradiance forecasting. *Renewable Energy* . 2023, vol. 209. DOI: 10.1016/j.renene.2023.03.122.

[32] WEN, H., et al. Deep Learning Based Multistep Solar Forecasting for PV Ramp-Rate Control Using Sky Images. *IEEE Transactions on Industrial Informatics*. 2021, vol. 17, no. 2. DOI: 10.1109/TII.2020.2987916.

[33] AL-LAHHAM, A., O. THEEB, K. ELALEM, ALSHAWI, S. A. ALSHEBEILI. Sky Imager-Based Forecast of Solar Irradiance Using Machine Learning. *Electronics*. 2020, vol. 9, no. 10. DOI: 10.3390/ELECTRONICS9101700.

[34] LORENZ, E., J. KÜHNERT, D. HEINEMANN. Short Term Forecasting of Solar Irradiance by Combining Satellite Data and Numerical Weather Predictions. *27th European Photovoltaic Solar Energy Conference and Exhibition*. 2012, pp. 4401–4405. DOI: 10.4229/27THEUPVSEC2012-6DO.12.1.

[35] MATHIESEN, P., J. KLEISSL. Evaluation of numerical weather prediction for intra-day solar forecasting in the continental United States. *Solar Energy*. 2011, vol. 85, iss. 5, pp. 967–977. DOI: 10.1016/J.SOLENER.2011.02.013.

[36] DUTT, V., S. SHARMA. 9 - Artificial intelligence and technology in weather forecasting and renewable energy systems: emerging techniques and worldwide studies. *Artificial Intelligence for Renewable Energy Systems*. 2022, pp. 189-207. DOI: 10.1016/B978-0-323-90396-7.00009-2.

[37] LAURET, P., M. DIAGNE, M. DAVID. A Neural Network Post-processing Approach to Improving NWP Solar Radiation Forecasts. *Energy Procedia*. 2014, vol. 57, pp. 1044–1052. DOI: 10.1016/J.EGYPRO.2014.10.089.

[38] XIE, Y., J. YANG, M. SENGUPTA, Y. LIU, X. ZHOU. Improving the prediction of DNI with physics-based representation of all-sky circumsolar radiation. *Solar Energy*. 2022, vol. 231, pp. 758–766. DOI: 10.1016/j.solener.2021.12.016.

[39] ARAUJO, J. M. S. D.. Performance comparison of solar radiation forecasting between WRF and LSTM in Gifu, Japan. *Environmental Research Communications* . 2020, vol. 2, no. 4. DOI: 10.1088/2515-7620/AB7366.

[40] VERBOIS, H., R. HUVA, A. RUSYDI, W. WALSH. Solar irradiance forecasting in the tropics using numerical weather prediction and statistical learning. *Solar Energy*. 2018, vol. 162, pp. 265–277. DOI: 10.1016/J.SOLENER.2018.01.007.

[41] VERBOIS, H., Y.-M. SAINT-DRENAN, A. THIERY, P. BLANC. Statistical learning for NWP post-processing: A benchmark for solar irradiance forecasting. *Solar Energy*. 2022, vol. 238, pp. 132–149. DOI: 10.1016/j.solener.2022.03.017.

[42] YANG, D., W. WANG, J. M. BRIGHT, C. VOYANT, G. NOTTON, G. ZHANG, C. LYU. Verifying operational intra-day solar forecasts from ECMWF and NOAA. *Solar Energy*. 2022, vol. 236, pp. 743–755. DOI: 10.1016/j.solener.2022.03.004.

[43] HUANG, J., L. RIKUS, Y. QIN, J. KATZFEY. Assessing model performance of daily solar irradiance forecasts over Australia. *Solar Energy*. 2018, vol. 176, pp. 615–6265. DOI: 10.1016/J.SOLENER.2018.10.080.

[44] ZHANG, G., D. YANG, G. GALANIS, E. ANDROULAKIS. Solar forecasting with hourly updated numerical weather prediction. *Renewable and Sustainable Energy Reviews*. 2022, vol. 154. DOI: 10.1016/j.rser.2021.111768.

[45] SHADAB, A., S. SAID, S. AHMAD. Box–Jenkins multiplicative ARIMA modeling for prediction of solar radiation: a case study. *International Journal of Energy and Water Resources*. 2019, vol. 3, pp. 305-–318. DOI: 10.1007/S42108-019-00037-5.

[46] WU, J., C. K. CHAN. Prediction of hourly solar radiation using a novel hybrid model of ARMA and TDNN. *Solar Energy*. 2011, vol. 85, iss. 5, pp. 808–817. DOI: 10.1016/J.SOLENER.2011.01.013.

[47] GUPTA, A., K. GUPTA, S. SAROHA. A review and evaluation of solar forecasting technologies. *Materials Today: Proceedings*. 2021, vol. 47, pp. 2420–2425. DOI: 10.1016/J.MATPR.2021.04.491.

[48] SHADAB, A., S. AHMAD, S. SAID. Spatial forecasting of solar radiation using ARIMA model. *Remote Sensing Applications: Society and Environment*. 2020, vol. 20. DOI: 10.1016/J.RSASE.2020.100427.

[49] SANSA, I., Z. BOUSSAADA, M. MAZIGH, N. M. BELLAAJ. Solar radiation prediction for a winter day using ARMA model. *2020 6th IEEE International Energy Conference (ENERGYCon), Gammarth, Tunisia*. 2020, pp. 326–330. DOI: 10.1109/ENERGYCon48941.2020.9236541.

[50] EL ALANI, O., C. HAJJAJ, H. GHENNIOUI, A. GHENNIOUI, P. BLANC, Y.-M. SAINT-DRENAN, M. EL MONADY. Performance assessment of SARIMA, MLP and LSTM models for short-term solar irradiance prediction under different climates in Morocco. *International Journal of Ambient Energy*. 2021, vol. 44, iss. 1, pp. 334–350. DOI: 10.1080/01430750.2022.2127889.

[51] ALSHARIF, M. H., M. K. YOUNES, J. KIM. Time Series ARIMA Model for Prediction of Daily and Monthly Average Global Solar Radiation: The Case Study of Seoul, South Korea. *Symmetry*. 2019, vol. 11, no. 2. DOI: 10.3390/SYM11020240.

[52] HAIDER, S. A., M. SAJID, H. SAJID, E. UDDIN, Y. AYAZ. Deep learning and statistical methods for short- and long-term solar irradiance forecasting for Islamabad. *Renewable Energy*. 2022, vol. 198. DOI: 10.1016/j.renene.2022.07.136.

[53] SANTOS, D. S. D. O., et al. Solar Irradiance Forecasting Using Dynamic Ensemble Selection. *Applied Sciences*. 2022, vol. 12, no. 7. DOI: 10.3390/app12073510.

[54] WATHMINI, S., F. LAKCHANI, K. AHILAN, V. RAGUPATHYRAJ, K. ANANTHARAJAH. Long-term Solar Irradiance Forecasting Approaches - A Comparative Study. *2018 IEEE International Conference on Information and Automation for Sustainability (ICIAfS), Colombo, Sri Lanka*. 2018. DOI: 10.1109/ICIAFS.2018.8913381.

[55] BELMAHDI, B., M. LOUZAZNI, A. EL BOUARDI. Comparative optimization of global solar radiation forecasting using machine learning and time series models. *Environmental Science and Pollution Research*. 2021, vol. 29, pp. 14871—14888. DOI: 10.1007/S11356-021-16760-8.

[56] BELMAHDI, B., M. LOUZAZNI, M. MARZBAND, A. EL BOUARDI. Global Solar Radiation Forecasting Based on Hybrid Model with Combinations of Meteorological Parameters: Morocco Case Study. *Forecasting*. 2023, vol. 5, no. 1. DOI: 10.3390/forecast5010009.

[57] PAULESCU, M., E. PAULESCU. Short-term forecasting of solar irradiance. *Renewable Energy*. 2019, vol. 143. DOI: 10.1016/J.RENENE.2019.05.075.

[58] WANG, F., Z. MI, S. SU, H. ZHAO. Short-Term Solar Irradiance Forecasting Model Based on Artificial Neural Network Using Statistical Feature Parameters. *Energies*. 2012, vol. 53, no. 5. DOI: 10.3390/EN5051355.

[59] SHARMA, V., S. RAI, A. DEV. A Comprehensive Study of Artificial Neural Networks. *Computer Science, Business*. 2012.

[60] YADAV, A. K., S. S. CHANDEL. Solar radiation prediction using Artificial Neural Network techniques: A review. *Renewable and Sustainable Energy Reviews*. 2014, vol. 33. DOI: 10.1016/J.RSER.2013.08.055.

[61] QAZI, A., H. FAYAZ, A. WADI, R. G. RAJ, N. A. Rahim, W. A. KHANL. The artificial neural network for solar radiation prediction and designing solar systems: a systematic literature review. *Journal of Cleaner Production*. 2015, vol. 104, pp. 1–12. DOI: 10.1016/J.JCLEPRO.2015.04.041.

[62] ZAFARI, A., M. H. KIANMEHR, R. ABDOLAHZADEH. Modeling the effect of extrusion parameters on density of biomass pellet using artificial neural network. *International Journal Of Recycling of Organic Waste in Agriculture*. 2013, vol. 2, no. 9. DOI: 10.1186/2251-7715-2-9.

[63] ÇOBAN, R., D. AVAN, Ö. ERÇİN. Dinamik sistem modelleme için yeni bir geri beslemeli sinir aği yaklaşimi.

[64] ARORA, I., J. GAMBHIR, T. KAUR. Data Normalisation-Based Solar Irradiance Forecasting Using Artificial Neural Networks. *Arabian Journal for Science and Engineering*. 2021, vol. 46, pp. 1333-–1343. DOI: 10.1007/S13369-020-05140-Y.

[65] MOHAMED, Z. E.. Using the artificial neural networks for prediction and validating solar radiation. *Journal of the Egyptian Mathematical Society*. 2019, vol. 27, no. 47. DOI: 10.1186/S42787-019-0043-8.

[66] KURNIAWAN, A., E. S. KOENHARDONO, I. R. KUSUMA, J. PRANANDA, S. SARWITO, A. A. MASROERI. An Estimation of hourly average solar radiation using artificial neural network in the city of Surabaya. *IOP Conference Series: Materials Science and Engineering*. 2020, vol. 1052. DOI: 10.1088/1757-899X/1052/1/012002.

[67] ARSLAN, G., B. BAYHAN, K. YAMAN. Mersin / Türkiye için Ölçülen Global Güneş Işınımının Yapay Sinir Ağları ile Tahmin Edilmesi ve Yaygın Işınım Modelleri ile Karşılaştırılması. *Fen Bilimleri Dergisi*. 2019, vol. 7, no. 1, pp. 80–96. DOI: 10.29109/gujsc.419473.

[68] ŞAHAN, M.. Yapay Sinir Ağları ve Angström-Prescott Denklemleri Kullanılarak Gaziantep, Antakya ve Kahramanmaraş İçin Global Güneş Radyasyonu Tahmini. *Araştırma Makalesi*. 2021, vol. 16, no. 2, pp. 368–384. DOI: 10.29233/sdufeffd.953182.

[69] ANTONOPOULOS, V. Z., D. PAPAMICHAIL, V. ASCHONITIS, A. V. ANTONOPOULOS. Solar radiation estimation methods using ANN and empirical models. *Computers and Electronics in Agriculture*. 2019, vol. 160, pp. 160–167. DOI: 10.1016/J.COMPAG.2019.03.022.

[70] BENALI, L., G. NOTTON, A. FOUILLOY, C. VOYANT, R. DIZENE. Solar radiation forecasting using artificial neural network and random forest methods: Application to normal beam, horizontal diffuse and global components. *Renewable Energy*. 2019, vol. 132, pp. 871–884. DOI: 10.1016/J.RENENE.2018.08.044.

[71] MARZOUQ, M., H. EL FADILI, K. ZENKOUAR, Z. LAKHLIAI, M. AMOUZG. Short term solar irradiance forecasting via a novel evolutionary multi-model framework and performance assessment for sites with no solar irradiance data. *Renewable Energy*. 2020, vol. 157, pp. 214–231. DOI: 10.1016/J.RENENE.2020.04.133.

[72] MARZOUQ, M., Z. BOUNOUA, A. MECHAQRANE, H. EL FADILI, Z. LAKHLIAI, K. ZENKOUAR. ANN-based modelling and prediction of daily global solar irradiation using commonly measured meteorological parameters. *IOP Conference Series: Earth and Environmental Science*. 2018, vol. 161. DOI: 10.1088/1755-1315/161/1/012017.

[73] AĞBULUT, Ü., A. E. GÜREL, Y. BIÇEN. Prediction of daily global solar radiation using different machine learning algorithms: Evaluation and comparison. *Renewable and Sustainable Energy Reviews*. 2021, vol. 135. DOI: 10.1016/J.RSER.2020.110114.

[74] ARIMAN, S., G. Y. TAFLAN, E. ÇELIK. Samsun Bölgesi için Güneş Radyasyonunun Yapay Sinir Ağı ile Tahmini. *Araştırma Makalesi*. 2021, vol. 25. DOI: 10.31590/EJOSAT.866139.

[75] SHINDE, P., S. SHAH. A Review of Machine Learning and Deep Learning Applications. *2018 Fourth International Conference on Computing Communication Control and Automation (ICCUBEA), Pune, India*. 2018. DOI: 10.1109/ICCUBEA.2018.8697857.

[76] MAHESH, B.. Machine Learning Algorithms - A Review. *International Journal of Science and Research (IJSR)*. 2020, vol. 9, iss. 1. DOI: 10.21275/ART20203995.

[77] D. H. W. LI, W. CHEN, S. LI, S. LOU. Estimation of hourly global solar radiation using Multivariate Adaptive Regression Spline (MARS) – A case study of Hong Kong. *Energy*. 2019, vol. 186. DOI: 10.1016/J.ENERGY.2019.115857.

[78] LI, J., J. WARD, J. TONG, L. COLLINS, G. PLATTG. Machine learning for solar irradiance forecasting of photovoltaic system. *Renewable Energy*. 2016, vol. 90, pp. 542–553. DOI: 10.1016/J.RENENE.2015.12.069.

[79] WANXIANG, Y., Z. CHUNXIAO, H. HAO, X. WANG, L. XIANLI. A support vector machine approach to estimate global solar radiation with the influence of fog and haze. *Renewable Energy*. 2018, vol. 128, pp. 155–162. DOI: 10.1016/J.RENENE.2018.05.069.

[80] KHOSRAVI, A., R. N. N. KOURY, L. MACHADO, J. J. G. PABON. Prediction of hourly solar radiation in Abu Musa Island using machine learning algorithms. *Journal of Cleaner Production*. 2018, vol. 176, pp. 63–75. DOI: 10.1016/J.JCLEPRO.2017.12.065.

[81] PEDRO, H. T. C., C. F. M. COIMBRA, M. DAVID, P. LAURET. Assessment of machine learning techniques for deterministic and probabilistic intra-hour solar forecasts. *Renewable Energy*. 2018, vol. 123, pp. 191–203. DOI: 10.1016/J.RENENE.2018.02.006.

[82] FAN, J., L. WU, X. MA, H. ZHOU, F. ZHANG. Hybrid support vector machines with heuristic algorithms for prediction of daily diffuse solar radiation in air-polluted regions. *Renewable Energy*. 2020, vol. 145, pp. 2034–2045. DOI: 10.1016/J.RENENE.2019.07.104.

[83] DEMIR, V., H. CITAKOGLU. Forecasting of solar radiation using different machine learning approaches. *Neural Computing and Applications*. 2022, vol. 35, pp. 887—906. DOI: 10.1007/s00521-022-07841-x.

[84] HUANG, L., J. KANG, J. KANG, M. WAN, L. FANG, C. ZHANG, Z. ZENG. Solar Radiation Prediction Using Different Machine Learning Algorithms and Implications for Extreme Climate Events. *Frontiers in Earth Science*. 2021, vol. 9. DOI: 10.3389/FEART.2021.596860.

[85] AYKO, O., S. B. KESER. A comparison of machine learning algorithms for forecasting solar irradiance in Eskişehir, Turkey. *International Journal of Applied Mathematics Electronics and Computers*. 2021, vol. 9, iss. 4, pp. 103–109. DOI: 10.18100/ijamec.995506.

[86] DEMOLLI, H., et al. Makine Öğrenmesi Algoritmalarıyla Güneş Enerjisi Tahmini: Niğde İli Örneği. *International Turkic World Congress on Science and Engineering*. 2019.

[87] BEKÇIOĞULLARI, M. F., et al. Güneş Enerjisinin Kısa-Dönem Tahmininde Farklı Makine Öğrenme Yöntemlerinin Karşılaştırılması. *Araştırma Makalesi*. 2021, vol. 11, iss. 22, pp. 37–45.

[88] VANDEVENTER, W., JAMEI, et al. Short-term PV power forecasting using hybrid GASVM technique. *Renewable Energy*. 2019, vol. 140, pp. 367–379. DOI: 10.1016/J.RENENE.2019.02.087.

[89] ONGSULEE, P.. Artificial intelligence, machine learning and deep learning. *2017 15th International Conference on ICT and Knowledge Engineering (ICT&KE), Bangkok, Thailand*. 2017. DOI: 10.1109/ICTKE.2017.8259629.

[90] EL NAQA, I., M. J. MURPHY. What are machine and deep learning?. *In: Machine and deep learning in oncology, medical physics and radiology. Cham: Springer International Publishing*. 2022. DOI: 10.1007/978-3-030-83047-2_1/COVER.

[91] JALALI, S. M. J., S. AHMADIAN, A. KAVOUSI-FARD, A. KHOSRAVI, S. NAHAVANDI. Automated Deep CNN-LSTM Architecture Design for Solar Irradiance Forecasting. *IEEE Transactions on Systems, Man, and Cybernetics: Systems*. 2022, vol. 52, no. 1, pp. 54–65. DOI: 10.1109/tsmc.2021.3093519.

[92] RAJAGUKGUK, R. A., R. A. A. RAMADHAN, H. LEE. A Review on Deep Learning Models for Forecasting Time Series Data of Solar Irradiance and Photovoltaic Power. *Energies*. 2020, vol. 13, no. 24. DOI: 10.3390/EN13246623.

[93] XIAO, Y., Y. YIN. Hybrid LSTM Neural Network for Short-Term Traffic Flow Prediction. *Information*. 2019, vol. 10, no. 3. DOI: 10.3390/INFO10030105.

[94] HU, Y., et al. Overcoming the vanishing gradient problem in plain recurrent networks. *arXiv preprint arXiv:1801.06105*. 2018.

[95] CHANDOLA, D., H. GUPTA, V. A. TIKKIWAL, M. K. BOHRA. Multi-step ahead forecasting of global solar radiation for arid zones using deep learningr. *Procedia Computer Science*. 2020, vol. 167, pp. 626–635. DOI: 10.1016/J.PROCS.2020.03.329.

[96] WENTZ, V. H., J. N. MACIEL, J. J. G. LEDESMA, O. H. A. JUNIOR. Solar Irradiance Forecasting to Short-Term PV Power: Accuracy Comparison of ANN and LSTM Models. *Energies*. 2022, vol. 15, no. 7. DOI: 10.3390/en15072457.

[97] QING, X., Y. NIU. Hourly day-ahead solar irradiance prediction using weather forecasts by LSTM. *Energy*. 2018, vol. 148, pp. 461–468. DOI: 10.1016/J.ENERGY.2018.01.177.

[98] MUHAMMAD, A., J. M. LEE, S. HONG, S.-J. LEE, E. H. LEE. Deep Learning Application in Power System with a Case Study on Solar Irradiation Forecasting. *2019 International Conference on Artificial Intelligence in Information and Communication (ICAIIC), Okinawa, Japan*. 2019, pp. 275–279. DOI: 10.1109/ICAIIC.2019.8668969.

[99] YU, Y., J. CAO, J. ZHU. An LSTM Short-Term Solar Irradiance Forecasting Under Complicated Weather Conditions. *IEEE Access*. 2019, vol. 7, pp. 145651–145666. DOI: 10.1109/ACCESS.2019.2946057.

[100] WOJTKIEWICZ, J., M. HOSSEINI, R. GOTTUMUKKALA, T. L. CHAMBERS. Hour-Ahead Solar Irradiance Forecasting Using Multivariate Gated Recurrent Units. *Energies*. 2019, vol. 12, no. 21. DOI: 10.3390/EN12214055.

[101] ASLAM, M., J.-M. LEE, H.-S. KIM, S.-J LEE, S. HONG. Deep Learning Models for Long-Term Solar Radiation Forecasting Considering Microgrid Installation: A Comparative Study. *Energies*. 2020, vol. 13, no. 1. DOI: 10.3390/EN13010147.

[102] BRAHMA, B., R. WADHVANI. Solar Irradiance Forecasting Based on Deep Learning Methodologies and Multi-Site Data. *Symmetry*. 2020, vol. 12, no. 11. DOI: 10.3390/SYM12111830.

[103] BAMISILE, O., A. OLUWASANMI, C. J. EJIYI, N. YIMEN, S. OBIORA, Q. HUANG. Comparison of machine learning and deep learning algorithms for hourly global/diffuse solar radiation predictions. *International Journal of Energy Research*. 2021. DOI: 10.1002/ER.6529.

[104] MISHRA, S., P. PALANISAMY. An Integrated Multi-Time-Scale Modeling for Solar Irradiance Forecasting Using Deep Learning. *arXiv:1905.02616*. 2023.

[105] KARA, A.. Uzun-Kısa Süreli Bellek Ağı Kullanarak Global Güneş Işınımı Zaman Serileri Tahmini. *Gazi Üniversitesi Fen Bilimleri Dergisi Part C: Tasarım ve Teknoloji*. 2019, vol. 7, no. 4, pp. 882–892. DOI: 10.29109/GUJSC.571831.

[106] MUKHOTY, B. P., V. MAURYA, S. K. SHUKLA. Sequence to sequence deep learning models for solar irradiation forecasting. *2019 IEEE Milan PowerTech, Milan, Italy*. 2019. DOI: 10.1109/PTC.2019.8810645.

[107] HUANG, X., C. ZHANG, Q. LI, Y. TAI, B. GAO, J. SHI. A Comparison of Hour-Ahead Solar Irradiance Forecasting Models Based on LSTM Network. *Mathematical Problems in Engineering*. 2020. DOI: 10.1155/2020/4251517.

[108] HOU, M., et al. Global Solar Radiation Prediction Using Hybrid Online Sequential Extreme Learning Machine Model. *Energies*. 2018, vol. 11, no. 12. DOI: 10.3390/EN11123415.

[109] BELMAHDI, B., M. LOUZAZNI, A. EL BOUARDI. A hybrid ARIMA–ANN method to forecast daily global solar radiation in three different cities in Morocco. *The European Physical Journal Plus*. 2020, vol. 135. DOI: 10.1140/EPJP/S13360-020-00920-9.

[110] HALABI, L. M., S. MEKHILEF, M. HOSSAIN. Performance evaluation of hybrid adaptive neuro-fuzzy inference system models for predicting monthly global solar radiation. *Applied Energy*. 2018, vol. 213. DOI: 10.1016/J.APENERGY.2018.01.035.

[111] ÁLVAREZ-ALVARADO, J. M., et al. Hybrid Techniques to Predict Solar Radiation Using Support Vector Machine and Search Optimization Algorithms: A Review. *Applied Sciences*. 2021, vol. 11, no. 3. DOI: 10.3390/APP11031044.

[112] EL ALANI, O., M. ABRAIM, H. GHENNIOUI, A. GHENNIOUI, I. IKENBI, F. DAHR. Short term solar irradiance forecasting using sky images based on a hybrid CNN–MLP model. *Applied Sciences*. 2021, vol. 7. DOI: 10.1016/J.EGYR.2021.07.053.

[113] SI, Z., Y. YU, M. YANG, P. LI. Hybrid Solar Forecasting Method Using Satellite Visible Images and Modified Convolutional Neural Networks. *IEEE Transactions on Industry*

Applications. 2021, vol. 57, no. 1, pp. 5–16. DOI: 10.1109/ICPS48389.2020.9176798.

[114] PALETTA, Q., G. ARBOD, J. LASENBY. Omnivision forecasting: Combining satellite and sky images for improved deterministic and probabilistic intra-hour solar energy predictions. *Applied Energy*. 2023, vol. 336. DOI: 10.1016/j.apenergy.2023.120818.

[115] KUMARI, P., D. TOSHNIWAL. Omnivision forecasting: Long short term memory–convolutional neural network based deep hybrid approach for solar irradiance forecasting. *Applied Energy*. 2021, vol. 295. DOI: 10.1016/J.APENERGY.2021.117061.

[116] GHIMIRE, S., R. C. DEO, D. CASILLAS-PÉREZ, S. SALCEDO-SANZ, E. SHARMA, M. ALI. Deep learning CNN-LSTM-MLP hybrid fusion model for feature optimizations and daily solar radiation prediction. *Measurement*. 2022, vol. 202. DOI: 10.1016/j.measurement.2022.111759.

[117] YAN, K., H. SHEN, L. WANG, H. ZHOU, M. XU, Y. MO. Short-Term Solar Irradiance Forecasting Based on a Hybrid Deep Learning Methodology. *Information*. 2020, vol. 11, no. 1. DOI: 10.3390/INFO11010032.

[118] JAIHUNI, M., et al. A Partially Amended Hybrid Bi-GRU—ARIMA Model (PAHM) for Predicting Solar Irradiance in Short and Very-Short Terms. *Energies*. 2020, vol. 13, no. 2. DOI: 10.3390/EN13020435.

[119] BENATIALLAH, D., K. BOUCHOUICHA, A. BENATIALLAH, A. HARROUZ, B. NASRI. Forecasting of Solar Radiation using an Empirical Model. *Algerian Journal of Renewable Energy and Sustainable Development*. 2019. DOI: 10.46657/AJRESD.2019.1.2.11.

[120] MAMUN, A. A., M. SOHEL, N. MOHAMMAD, M. S. HAQUE SUNNY, D. R. DIPTA, E. HOSSAIN. A Comprehensive Review of the Load Forecasting Techniques Using Single and Hybrid Predictive Models. *IEEE Access*. 2020, vol. 8, pp. 134911–134939. DOI: 10.1109/ACCESS.2020.3010702.

[121] HUANG, C., L. CAO, N. PENG, S. LI, J. ZHANG, L. WANG, X. LUO, J.-H. WANG. Day-Ahead Forecasting of Hourly Photovoltaic Power Based on Robust Multilayer Perception. *Sustainability*. 2018, vol. 10, no. 12. DOI: 10.3390/SU10124863.

[122] DE GUIA, J. D., R. S. CONCEPCION, H. A. CALINAO, J. ALEJANDRINO, E. P. DADIOS, E. SYBINGCO. Using Stacked Long Short Term Memory with Principal Component Analysis for Short Term Prediction of Solar Irradiance based on Weather Patterns. *2020 IEEE REGION 10 CONFERENCE (TENCON), Osaka, Japan*. 2020, pp. 946-951. DOI: 10.1109/TENCON50793.2020.9293719.

[123] HAJIRAHIMI, Z., M. KHASHEI. Hybridization of hybrid structures for time series forecasting: a review. *Artificial Intelligence Review*. 2022, Vol. 56, pp. 1201—1261. DOI: 10.1007/s10462-022-10199-0.

[124] ALMARAASHI, M.. Investigating the impact of feature selection on the prediction of solar radiation in different locations in Saudi Arabia. *Applied Soft Computing*. 2018, Vol. 66, pp. 250–263. DOI: 10.1016/J.ASOC.2018.02.029.

[125] SEVAS, M. S., N. J. SHARMIN, C. F. T. SANTONA, S. R. SAGOR. Advanced ensemble machine-learning and explainable ai with hybridized clustering for solar irradiation prediction in Bangladesh. *Theoretical and Applied Climatology*. 2024, Vol. 155, pp. 5695—5725. DOI: 10.1007/s00704-024-04951-5.

[126] CHAIBI, M., EL M. BENGHOULAM, L. TARIK, M. BERRADA, A. El HMAIDI. An Interpretable Machine Learning Model for Daily Global Solar Radiation Prediction. *Energies*. 2021, Vol. 14, no. 21. DOI: 10.3390/EN14217367.

[127] ALMARAASH, M., M. ABDULRAHIM, H. HAGRAS. A Life-Long Learning XAI Metaheuristic-Based Type-2 Fuzzy System for Solar Radiation Modeling. *IEEE Transactions on Fuzzy Systems*. 2024, vol. 32, no. 4, pp. 2102–2115. DOI: 10.1109/tfuzz.2023.3343955.

[128] PRASAD, S. S.. Solar ultraviolet radiation predictions under cloud cover effects with artificial intelligence approaches. *University of Southern Queensland*. 2023. DOI: 10.26192/z3qq0.

[129] GONÇALVES, C., R. J. BESSA, P. PINSON. Privacy-Preserving Distributed Learning for Renewable Energy Forecasting. *IEEE Transactions on Sustainable Energy*. 2021, vol. 12, no. 3, pp. 1777–1787. DOI: 10.1109/TSTE.2021.3065117.

[130] LU, Y., L. WANG, C. ZHU, L. ZOU, M. ZHANG, L. FENG, Q. CAO. Predicting surface solar radiation using a hybrid radiative Transfer–Machine learning model. *Renewable and Sustainable Energy Reviews*. 2023, vol. 173. DOI: 10.1016/j.rser.2022.113105.

[131] NIU, T.-X., J. LI, W. WEI, H. G. YUE. A hybrid deep learning framework integrating feature selection and transfer learning

for multi-step global horizontal irradiation forecasting. *Applied Energy*. 2022, vol. 326. DOI: 10.1016/j.apenergy.2022.119964.

[132] PUAH, B. K., L. W. CHONG, Y. W. WONG, K. M. BEGAM, N. KHAN, M. A. JUMAN, R. K. RAJKUMAR. A regression unsupervised incremental learning algorithm for solar irradiance prediction. *Renewable Energy*. 2021, vol. 164. DOI: 10.1016/J.RENENE.2020.09.080.

[133] BAI L., et al. Predictability and forecast skill of solar irradiance over the contiguous United States. *Renewable and Sustainable Energy Reviews*. 2023, vol. 182. DOI: 10.1016/j.rser.2023.113359.

[134] GERGES, F., M. C. BOUFADEL, E. BOUZEID, H. NASSIF, J. T. L. WANG. Long-term prediction of daily solar irradiance using Bayesian deep learning and climate simulation data. *Knowledge and Information Systems*. 2023, Vol. 66, pp. 613-–633. DOI: 10.1007/s10115-023-01955-x.

[135] NWOKOLO, S. C., J. C. OGBULEZIE, O. J. USHIE. A multi-model ensemble-based CMIP6 assessment of future solar radiation and PV potential under various climate warming scenarios. *Optik*. 2023, Vol. 285. DOI: 10.1016/j.ijleo.2023.170956.